Open Access Library Journal
2023, Volume 10, e10482
ISSN Online: 2333-9721
ISSN Print: 2333-9705

Piezoelectric Actuators Application and Hysteresis Modelling: A Brief Survey

Yazhou Yang

School of Communication and Electronic Engineering, Jishou University, Jishou, China
Email: 1010196312@qq.com

How to cite this paper: Yang, Y.Z. (2023) Piezoelectric Actuators Application and Hysteresis Modelling: A Brief Survey. *Open Access Library Journal*, **10**: e10482.
https://doi.org/10.4236/oalib.1110482

Received: July 6, 2023
Accepted: August 8, 2023
Published: August 11, 2023

Abstract

In modern life and production, there exists a global energy crisis, an increasing demand for advanced medical services, and a need to integrate and miniaturize industrial products. The applications based on conventional actuators struggle to cope with crises and growing demands due to their low resolution. To address the above issues, researchers have been working on and developing the excellent properties of piezoelectric materials since the discovery of the piezoelectric effect. Nowadays, piezoelectric actuators (PEAs), which are based on piezoelectric materials, have become widely utilized in energy harvesting, micro-electro-mechanical systems (MEMS), biomedicine and other fields. The control accuracy of PEAs in applications is limited by the inherent hysteresis nonlinearity, which poses a challenge to their applications. Researchers are working on PEAs and their hysteresis models to better serve humans with PEAs. This paper reviews typical applications and classifications of PEAs, typical hysteresis models, and classifications. At the end of the paper, we summarize the steps of the selective hysteresis modelling of PEAs and indicate the critical points of the hysteresis modelling and future research directions. The present paper provides a comprehensive review of classical hysteresis models and PEAs, which is expected to benefit researchers in the field of piezoelectric applications and efficient hysteresis modelling.

Subject Areas

Piezoelectric Hysteresis

Keywords

Piezoelectric Applications, Piezoelectric Hysteresis Modelling, Piezoelectric Actuators

1. Introduction

To solve the global energy scarcity crisis and serious pollution of the ecological

environment, and caused by the increase in non-renewable energy consumption [1], to cope with people's high requirements for medical treatment [2], the nanoscale resolution requirements of nano-positioning systems in industrial domains, and the requirements of users for high performance, easy to use, reliability and low cost of industrial products [3] [4]. Traditional fluid, electric, hydraulic, pneumatic, and electromagnetic actuators are challenging to achieve micron/nanometre resolution due to the limitations of the driving source and its volume [5]. Since the discovery of the piezoelectric effect by Curie *et al.* [6] in 1880, researchers have discovered properties of piezoelectric materials such as high resolution, elevated accuracy, rapid response, low power consumption, tiny size and flexible structural design [7]. Over time, researchers have developed piezoelectric single crystal, piezoelectric polycrystal (ceramic), piezoelectric polymer, piezoelectric polymer composite materials [8], and PEAs based on the utilization of high-performance piezoelectric materials is prevalent in the field of energy harvesting, MEMS, and biomedicine [9]. **Figure 1** illustrates different examples of applications of different PEAs. Various applications based on PEAs provide higher efficiency for human production and life. The study of PEAs is essential for better applications. Furthermore, the immanent hysteresis of PEAs, which is characterized by nonlinear behaviors based on piezoelectric materials can affect the control accuracy of PEAs. Therefore, the study of PEAs' hysteresis modelling is fundamental to obtaining high-precision hysteresis models of PEAs. It also provides the necessary conditions for high-precision control of PEAs.

The subsequent sections of the paper are structured as follows. The typical applications of PEAs and the characteristics of various PEAs have been described in Section 2. The typical hysteresis models of a PEAs are presented in Section 3. The general steps for the hysteresis modelling of PEAs have been given in Section 4. The main findings of this paper and points out future innovative directions for high-precision hysteresis modelling have been summarized in Section 5.

2. The Applications of PEAs

This section presents a comprehensive overview of the common applications of PEAs, including their application background, current status, and operating principles. Additionally, it introduces and classifies the commonly used PEAs in typical applications.

2.1. Applications

The typical applications of PEAs in the fields of energy harvesting, MEMS, biomedicine are first presented, and classifies piezoelectric materials according to their molecular complexity. As shown in **Figure 1**, it is divided into piezoelectric single crystal [26] [27], piezoelectric ceramic [28] [29], piezoelectric polymer [30], piezoelectric polymer composite materials [31]. This paper provides readers with a demand-oriented understanding of PEAs, and the introduction of their common applications serves as a reference for researchers.

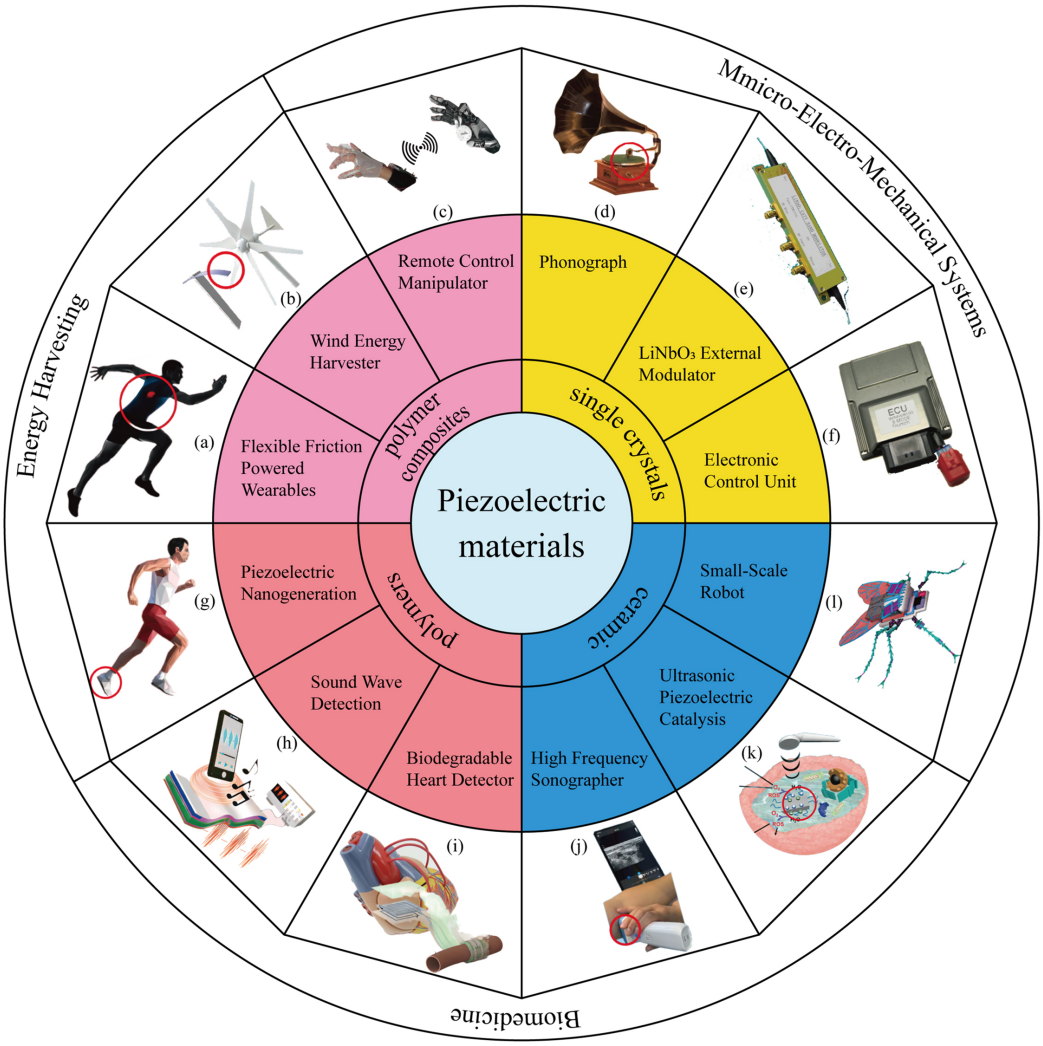

Figure 1. Common applications of piezoelectric materials. (a) Piezoelectric nanogenerator [10] [11]. (b) Flexible-friction powered wearables [12] [13]. (c) Wind energy harvester [14]. (d) Remote control manipulator [15] [16]. (e) Phonograph [17]. (f) LiNbO3 external modulator [18]. (g) Electronic control unit [19]. (h) Small scale robot [20]. (i) Ultrasonic piezoelectric catalysis [21]. (k) Biodegradable heart detector [22]. (j) High-frequency sonographer [23] [24]. (l) Sound wave detection [25].

2.1.1. Energy Harvesting

Vibrational energy is also widely found in buildings, human bodies, and vehicles. In order to collect a large amount of mechanical energy, researchers adopted a cantilever energy collector. Then they developed piezoelectric nano powered shoes with piezoelectric plates embedded in the sole, as shown in **Figure 1(a)** [1] [32].

For energy harvesting, researchers use PEAs to capture mechanical energy from living and natural environments and convert it into electrical energy. Because of conventional wind, hydroelectric and solar power, such technological devices are large, expensive and unsuitable for electronic power supplies. Existing chemical batteries provide unsustainable power and are difficult to recycle. To this end, researchers have developed friction nanogenerators suitable for re-

covering mechanical energy from human movement and life. As shown in **Figure 1(b)**, wearable electronic products made of multi-layer flexible piezoelectric materials worn by humans will produce friction when they move [6]. And friction nanogenerators are also self-contained power sources for wearable electronics [33].

The environmentally friendly wind energy is abundantly available in nature. Traditional wind conversion devices are not suitable for power micro devices due to their large volume and elevated cost. For researchers, piezoelectric harvesters have been developed to convert wind energy into electricity through mechanical structures [5]. To that end, researchers have developed piezoelectric wind harvesters, which converts wind-to-electricity energy. **Figure 1(c)** illustrates the fundamental principle of the piezoelectric wind energy harvester [34]. Researchers will utilize wind turbines to harness natural wind energy and convert it into kinetic energy for rotational motion. When a windmill blade contacts a piezoelectric cantilever, it bends the cantilever and creates vibrations and voltages.

2.1.2. MEMS Systems

Recently, with the development of interactive human-machine interfaces in MEMS, it is important to control the machine more accurately and collect the feedback information of the machine. Researchers have developed bending angle piezoelectric sensors made of flexible piezoelectric materials. As shown in **Figure 1(d)**, sensors based on flexible piezoelectric materials are embedded in the manipulator, which can transmit commands and feedback to the manipulator's motion state in real-time in the two-way electronic system of human-machine interaction [7].

In order to enrich the recreational life of the people by recording sound, Edison [35] invented the phonograph. As shown in **Figure 1(e)**, researchers used ageing-resistant piezoelectric single crystals for phonograph pickup. When the record is flipped, the stylus produces different deformations depending on the texture of the record, which then generate different currents that pass through the microphone to produce sound waves [36].

In the information age, researchers have been devoted to rapid data transmission. The currently available frequency-stable lasers with narrow linewidth exhibit exceptional properties and enjoy widespread utilization. However, to additionally achieve the requirements of narrower linewidth and faster frequency control, researchers have developed a modulator using lithium niobate chip. As shown in **Figure 1(f)**, the lithium niobate external modulator developed by researchers has less noise and lower voltage than the conventional modulator [9] [37]. MEMS are widely used in human production and life to improve their integration and miniaturization. The researchers used quartz crystal tuning forks as piezoelectric resonators to time MEMS. As shown in **Figure 1(g)**, the electronic control unit adopts a tuning fork crystal resonator to time and generate clock frequency signals [38]. Robots have experienced significant growth in re-

cent years. However, their effectiveness is limited in certain specialized situations such as disaster site search and rescue, infrastructure monitoring, and reconnaissance missions. In addition, the robot is limited by traditional actuators' size and manufacturing process. Therefore, the field of microrobots in MEMS has become a research hotspot [39]. As shown in **Figure 1(h)**, researchers use piezoelectric materials as fly wings [11]. The piezoelectric material vibrates fast at high frequency and outputs enough vibration force to meet the requirements of the miniature robotic fly wing.

2.1.3. Biomedicine

As medical research deepens and more advanced medical devices become available, the level of awareness of malignant tumour-related diseases among medical workers is also improving. Current techniques for inducing apoptosis of tumour cells by reactive oxygen species are highly dependent on oxygen in the tumour microenvironment. Therefore, how to generate oxygen in the tumour microenvironment is key to efficient apoptosis of tumour cells. To induce specific cell apoptosis in cancer therapy, barium titanate nanoparticles have been developed based on ultrasonic catalysis and hydrolysis. As shown in **Figure 1(i)**, ultrasonic piezoelectric catalysis is mainly used in the medical field, and ultrasonic stress-induced asymmetric piezoelectric catalysis of BaO_3Ti nanoparticles is used to treat hypoxic tumours [21] [40].

The internal complexity of living organisms limits the diagnosis and treatment of patients in modern medicine. Researchers have developed ultrasound detectors for medical imaging to assist doctors in diagnosing diseases. Next, the working principle of ultrasonic PEA is introduced. A sound wave is a form of energy transfer of an object in a mechanical vibrational state. The piezoelectric ultrasound transducer exploits the acoustic transmission properties of the object in the mechanical vibrational state to realize the mutual conversion of mechanical and electrical energy [41]. As shown in **Figure 1(j)**, the principle of a high-frequency ultrasonic instrument is to generate a high-frequency vibration wave by using the piezoelectric effect and then analyse the received vibration wave by using inverse piezoelectric effect and combine it with image processing to obtain the internal detection map of the object [23]. The piezoelectric materials that generate vibration are mainly $KNbO_3$-based single crystals [42].

Human health and longevity are limited by heart disease, which accounts for one in three deaths worldwide. The most direct and effective way to treat patients with heart disease is with an electronic device implanted in the heart. However, when the battery of an implantable electronic device is depleted, the surgical replacement of the battery poses a significant risk and financial burden to the patient. As a result, researchers have used flexible piezoelectric materials and biodegradable materials to develop self-powered heart monitoring devices attached to human blood vessels [43]. It converts vibrational energy generated by the human body into PEAs and continuously stores it as electrical energy to power heart monitoring devices. As shown in **Figure 1(k)**, the heart detector can

monitor the heart status in real-time [44]. The heart detector is mainly attached to the human heart by biodegradable flexible piezoelectric materials and is self-powered in the human body.

Deaf individuals experience challenges in communication due to the impairment or absence of cochlear hair cells. Existing cochlear implants struggle to recognize hearing in multiple sound sources. To this end, researchers have developed flexible, high-precision, high-sensitivity sound detection and recognition sensors [45]. As shown in **Figure 1(l)**, there is a flexible piezoelectric sensor in the acoustic sounder, which is mainly composed of flexible poly (vinylidenefluoride-co-trifluoroethylene) (PVDF-TrFE) piezoelectric sheets [25] [46].

In addition to energy harvesting, biomedicine, MEMS, and PEAs are widely utilized in aerospace, precision machining, optical manipulation, and numerous more advanced technologies. With the extensive range of applications of PEAs in precision engineering, engineers and technicians are demanding higher accuracy in PEAs modelling [47] [48]. The distinct characteristics of PEAs vary according to their types. To understand more about PEAs, the following sections further describe typical PEAs.

2.2. PEAs

In addition to the typical applications of PEAs mentioned in the previous section, various types of PEAs are widely employed in precision engineering due to their higher requirements for integration and control accuracy [49] [50] [51], which facilitates researchers in the field of precision control. PEAs are categorized in this section, and their fundamental operational principles are introduced. As shown in **Figure 2**. In this manuscript, PEAs are categorized into conventional actuators, piezoelectric stepping actuators, and multi-degree of freedom (MDOF) actuators based on their design and functionality [52]. The comprehensive types of PEAs mentioned in this section are highly informative for application design and meaningful for further development of PEAs.

2.2.1. Traditional PEA

As depicted in **Figure 2(a)**, conventional PEAs can be categorized into five types. The joint construction of unimorph PEAs involves the insertion of square, circular, annular or cantilevered unimorphs into a multilayer conducting metal electrode.

Different actuators may undergo shrinkage, expansion or bending in their designated driving directions due to the varying orientations of electric field and polarization, as illustrated in **Figure 2(b)**. Bimorph actuators are composed of two layers of piezoelectric material, each potentially attached to a metal gasket depending on the situation. Consequently, bimorph actuators can also be stretched/contracted or bent.

In **Figure 2(c)**, the piezoelectric tube actuator is formed by longitudinally polarizing a thin cylindrical piezoelectric material and bonding it to an electrode layer. Moreover, the piezoelectric tube actuators can be driven in axial/radial or transverse directions.

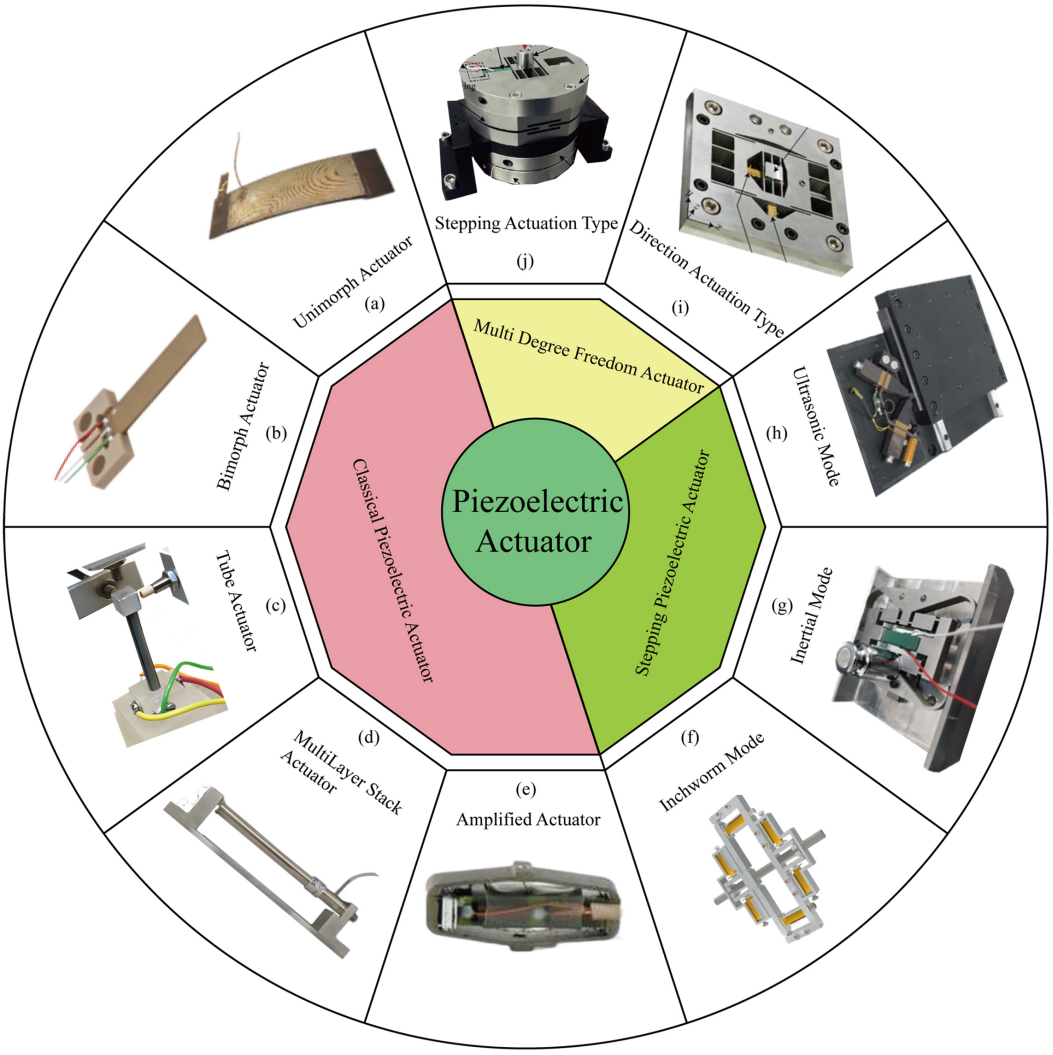

Figure 2. Category of PEAs. (a) Thunder actuator [53] [54]. (b) Bimorph piezoelectric actuator (PEA) [55] [56]. (c) Piezoelectric tube actuator [57] [58]. (d) Piezoelectric stack actuator [59] [60]. (e) Amplified PEA [61]. (f) Piezoelectric ceramics inchworm actuator [62]. (g) Inertial piezoelectric actuator [63]. (h) V-shaped linear ultrasonic actuator [64]. (i) Series-Paralle XY-Z PEA [65]. (j) Linear-Rotary inchworm PEA [66].

In **Figure 2(d)**, the multilayer piezoelectric stack actuator drivers employ multiple layers of piezoelectric material stacked on top of each other, with appropriate insulation separating the electrodes. Each layer is solely composed of piezoelectric material, and an electrode layer of the same polarity is connected to the external electrode. The driving range of these drivers varies from a few micrometres to tens of micrometres, while their driving force ranges from hundreds to thousands of newtons [67]. By applying different electric fields to the various piezoelectric layers, multilayer piezoelectric stack actuators can achieve more degrees of freedom and allow for longitudinal or shear displacements [68].

In **Figure 2(e)**, the amplified PEA consists of a bending hinge or compliant mechanism with stacked piezoelectric materials, depending on the design [69]. The elastic deformations generated by the amplified PEAs enable amplified motion to be achieved.

2.2.2. Stepping PEAs

In **Figure 2(f)**, the piezoelectric stepper actuator is capable of producing continuous linear or rotational motion that satisfies the requirements for extensive range and high precision in manipulator applications [60]. Based on either a stack PEA or an amplified PEA as the power source, researchers have proposed an inchworm-inspired PEA that utilizes the crawling principle for clamping feed stepping [70]. To achieve precise control over a wide range, they employ the inchworm-inspired PEA featuring an alternating gripping and driving mechanism. The most commonly utilized types include thrust-type actuators with fixed positions and walking-type actuators with moving positions [71].

In **Figure 2(g)**, the inertial PEAs, also referred to as stick-slip actuators, are depicted. are typically driven by sawtooth waves [72]. These actuators harness the energy generated by the deformation of piezoelectric materials through inertial and frictional forces. Based on different driving modes, researchers have classified them into two types: impact-driven and friction-driven. The former utilizes inertia to displace loads with the aid of static friction force and rapid contraction between loads [73]. The latter, known as a stick-slip PEA, generates its driving force by utilizing the difference in friction during stick-slip motion and rapid contraction [74].

The utilization of impact-type load inertia deviates from the primary characteristics of friction-type as depicted in **Figure 2(h)**. The ultrasonic PEA is primarily distinguished by its employment of high-frequency ultrasonic resonance drive, which endows it with exceptional speed and a broad range of continuous motion. The ultrasonic PEA propels the piezoelectric material to generate high-frequency vibrations through voltage waveforms of travelling and standing waves, which in turn drives the elastic stator on the piezoelectric material to produce an elliptical trajectory. Ultimately, this stator conducts high-frequency excitation ultrasonic waves to either a slider or rotor. The aforementioned process facilitates the implementation of linear and rotational motion with the structure of the piezoelectric ultrasonic actuator [75].

2.2.3. Multi Degree Freedom PEAs

In **Figure 2(i)**, the MDOF PEA can be connected in series or parallel with a single degree of freedom PEA, stacked PEA, or amplified PEA at a perpendicular angle to each other. Then, depending on the required degree of freedom, a hinge or flexible mechanism is designed to enable MDOF linear or rotational motion. Due to the different actuation modes, MDOF PEAs can be classified into two types: direct actuation and step actuation [76] [77]. The direct-drive MDOF PEAs offer high accuracy as an advantage, yet their range of motion is limited due to the utilization of multi-layer PEAs.

In **Figure 2(j)**, inchworm and ultrasonic actuators are commonly used in series or parallel to design multiple degrees of freedom (MDOF) stepping PEAs, which enable a more comprehensive range of motion. The accuracy and travel range of MDOF stepper PEAs depend on the type, precision, and arrangement of the PEAs [78].

The typical actuator of this section is used as the foundation mechanism in a typical application shown in **Figure 1**. In designing a PEA, the first step is determining the type of piezoelectric material and using a set of constants to assess whether the chosen piezoelectric material can achieve the desired performance. Second, researchers design the mechanism of the PEA and then study the modelling of the PEA [79]. Researchers have sought to better utilize piezoelectric materials in the fields of sensing and micromanipulation. Numerous studies have been conducted on the modelling of PEAs. However, the hysteresis nonlinearity of PEAs limits their application in precision engineering [1] [80].

3. Hysteresis Models

The positioning error of practical PEAs can be attributed to either rate-independent or rate-dependent hysteresis, with a maximum magnitude of 15% of the stroke range [81]. To enhance the utilization of PEAs, a comprehensive depiction of the hysteresis model is presented. Hysteresis nonlinearity is an characteristics of piezoelectric materials, and other properties such as multiple mapping, memory, and rate dependence further complicate accurate mathematical modelling of hysteresis characteristics [82]. The nonlinear hysteresis and creep of piezoelectric materials can generate stochastic oscillations, which pose a challenge to their application in high-precision micro displacement systems. Given that piezoelectric devices are utilized for high-precision positioning in dynamic scenarios, the modelling accuracy of a nonlinear dynamic hysteresis system is the primary determinant of its robustness [81] [83] [84]. The non-local memory, consisting of instantaneous input voltage value, historical voltage value, and historical voltage extreme value, exerts an influence on the current output displacement. Moreover, the hysteresis characteristics of piezoelectric materials can be categorized into rate-independent or rate-dependent hysteresis based on input frequency. The nonlinear hysteresis of the PEA is depicted in **Figure 3**, where **Figure 3(a)** illustrates the voltage input waveform, **Figure 3(b)** presents the relationship between voltage amplitude and output displacement, and **Figure 3(c)** displays different frequency hysteresis loops at identical voltage. The imprecise control of PEAs results in a system error that can reach up to 15% of its

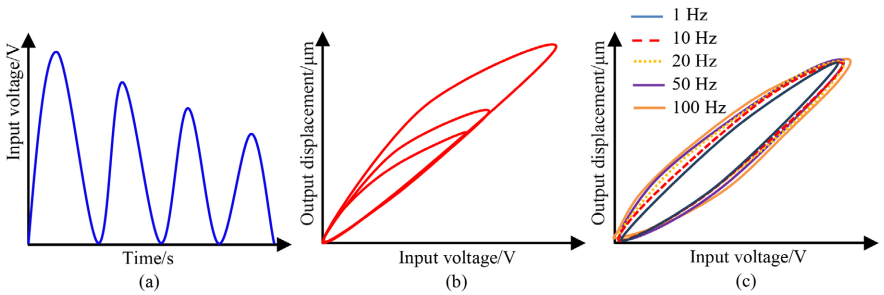

Figure 3. Major hysteresis loop of the piezoelectric micro positioning stage [86]. (a) Driving voltage waveform. (b) Relationship between driving voltage amplitude and output displacement. (c) Different frequency hysteresis loops.

stroke. Therefore, scholars are currently focusing on hysteresis modelling and control, as well as further compensation techniques to minimize errors [85]. Hysteresis modelling of PEAs can be broadly classified into two categories: classical basic models and advanced models. Classical hysteresis modelling has been further divided by researchers into phenomenological and physical models based on the macroscopic and microscopic states of piezoelectric materials. Although numerous researchers have made enhancements to the classical model, the focus of this section is to provide readers with a fundamental understanding of the classical model.

3.1. Phenomenological Models

The phenomenon model employs the black-box principle to represent a phenomenon that is either entirely unknown or partially known within a system composed of piezoelectric elements. A mathematical model is developed to capture the mapping relationship between external input and output, thereby accurately fitting the system. Parameters identification method is utilized to determine the unknown parameters and obtain the input or output model. Phenomenon models can be categorized into operator-based, differential equation-based, and rate-dependent models, as illustrated in **Figure 4**. The Preisach model [87], the Krasnosel' Skii-Pokrovskii (KP) model [88], and the Prandtl-Ishlinskii (PI) model all belong to the class of operators and are rate-independent. The Duhem, Backlash-like, and Bouc-Wen models are differential equation-based models. In addition, the Dahl model and Polynomial Model are classified as phenomenological models.

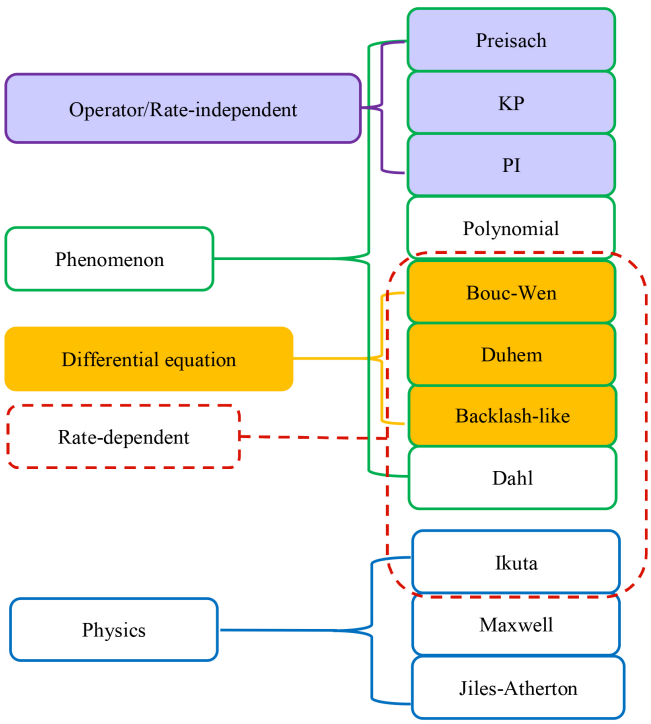

Figure 4. Category of classical hysteresis models for PEAs [81].

3.1.1. Preisach Model

After F. Preisach [87] proposed the Preisach model, Krasnosel'skii [88] developed it into a pure mathematical model, and Mayergoyz [89] further generalized it based on its characteristics. The Preisach model is derived from the superposition of relay operators, and the resulting curve can be utilized to depict the hysteresis phenomenon exhibited by PEAs. The nonideal relay operator formula is as follows.

$$y(x)=\begin{cases}1 & \text{if } x\geq\beta\\ 0 & \text{if } x\leq\alpha\\ k & \text{if } \alpha<x<\beta\end{cases} \tag{1}$$

This definition of the hysteron indicates that the current value of the complete hysteresis loop is contingent upon the historical record of variable input. The Relay operator of the convention Preisach model is shown in **Figure 5**. Because the history value of the hysteresis is nonlinear or the value of the previous position impacts the next output value, the local memory property. Furthermore, when $A<x_0<x<x_1<C$, the displacement is output according to the path of the red line segment, and the nonideal relay operator also has the local memory property.

The convention Preisach model is represented by N relay operators with weights in parallel [92] [93]. The formula is as follows.

$$y(t)=\iint_{\alpha\geq\beta}\mu(\alpha,\beta)R_{\alpha\beta}x(t)\mathrm{d}\alpha\mathrm{d}\beta \tag{2}$$

One of the most straightforward approaches to comprehending the Preisach model is through a geometric interpretation assignment to the coordinate plane (α,β). On this plane, each point (α_i,β_i) is associated wit a specific relay hysteron $R_{\alpha i},R_{\beta i}$.

Each relay can be represented on this so-called Preisach plane with its values [94]. As shown in **Figure 6** various trajectories can be obtained by stacking different weights with different rely operators. Then the curve is fitted to simulate the nonlinear hysteresis behaviour of the PEAs.

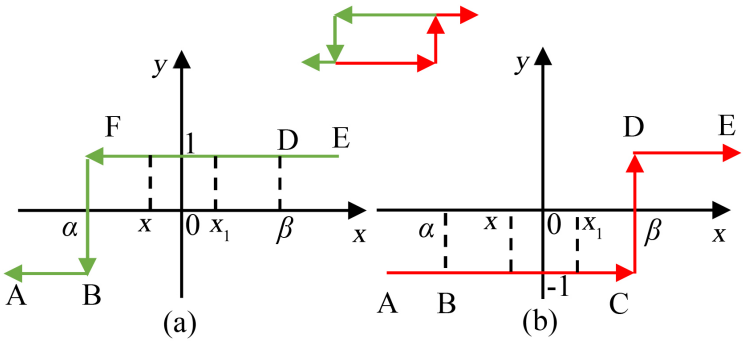

Figure 5. Fundamental switching (relay) operator-hysteron [90] [91]. (a) The left-direction trajectory of the relay operator. (b) The right-direction trajectory of the relay operator.

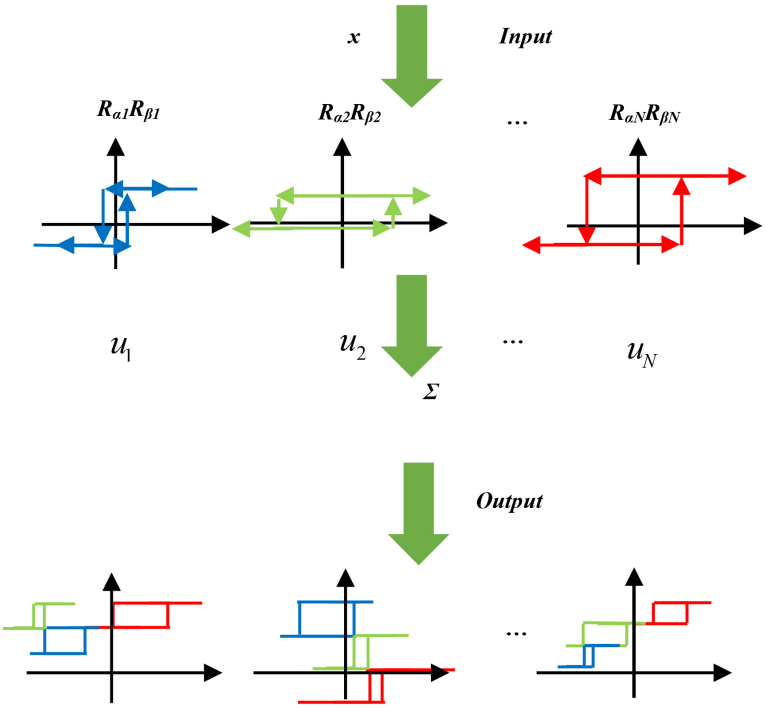

Figure 6. The different rely operator superimposes different trajectories [92] [95].

3.1.2. KP Model

Due to the complexity of solving the double integral in the Preisach model, KP model was developed by Bank *et al.* [96] The KP operator was established based on reliability and a superposition method was employed instead of integration. The KP operator is depicted in **Figure 7** [97].

The KP model is expressed as follows [100] [101] [102] [103].

$$x(t) = \int_S \left[k_p(v, \xi_S)\right](t) \mathrm{d}\mu(s) \tag{3}$$

where $k_p(v, \xi_S)$ expresses the KP operator as follows.

$$\left[k_p(v, \xi_S)\right](t) = \begin{cases} \min\left(\xi_S, r(v - s_1)\right) & \dot{v}(t) < 0 \\ \max\left(\xi_S, r(v - s_2)\right) & \dot{v}(t) > 0 \\ k_{p0} & \dot{v}(t) = 0 \end{cases} \tag{4}$$

where $v(t)$ is the input voltage, $x(t)$ is displacement output, S is the integral domain.

3.1.3. PI Model

PI model is an improvement of Prandtl and Krasnosel 'skii *et al.* [104] [105] based on Preisach model. PI model is characterized by the inclusion of play operator or stop operator. As shown in **Figure 8**, the PI model principle approximates the mass-spring system. Play operator is defined by.

$$y_r(t) = H_r\left[v(t), y_0\right] = \max\left\{v(t) - r, \min\left\{v(t) + r, y_r\left(t^-\right)\right\}\right\} \tag{5}$$

where H_r is the play operator and the threshold is r, $y_r\left(t^-\right)$ is the output at

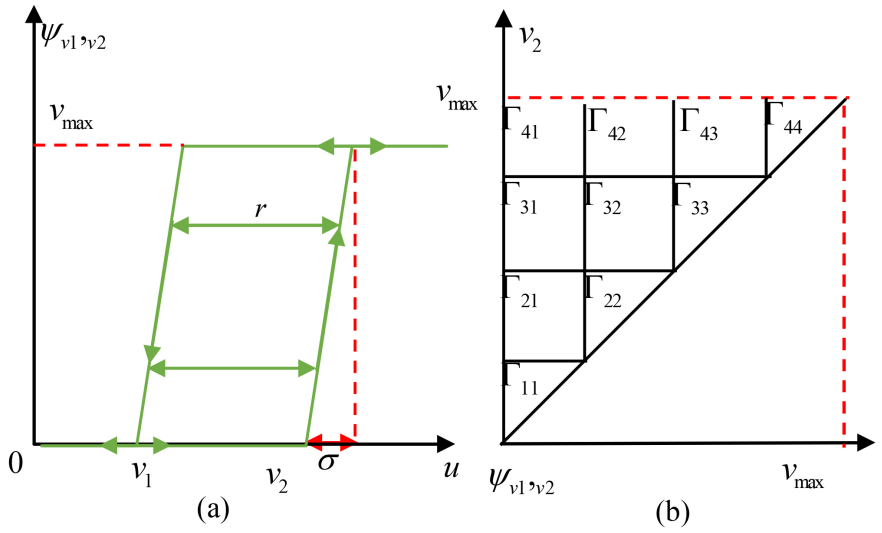

Figure 7. KP model. (a) Fundamental KP operator [98]. (b) Preisach plane and L = 4 [99].

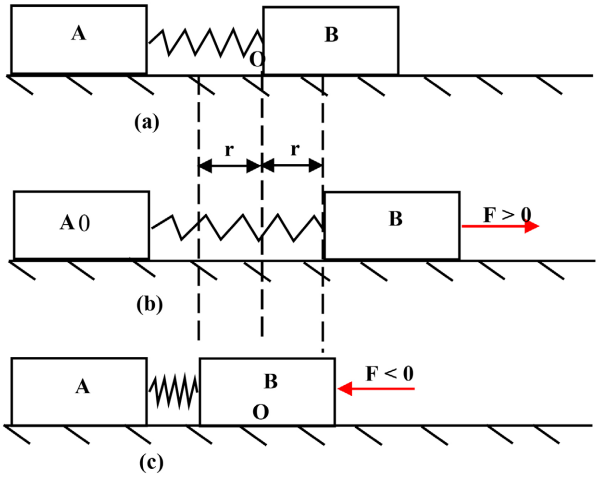

Figure 8. Spring-mass model is used to demonstrate Play operator. (a) Initial State. (b) B is moving to the right. (c) B is moving to the left [106] [107].

the last moment; $v(t)$ is the input; $y_r(t^-)$ is the output; initial value is y_0. PI model is expressed as a weighted sum of finite play operators.

So it is as follows.

$$y(t)=\omega^{\mathrm{T}}H_r\left[v(t),y_0\right]=\sum_{i=0}^{n}\omega_i\max\left\{v(t)-r_i,\min\left\{v(t)+r_i,y_i\left(t^-\right)\right\}\right\} \quad (6)$$

where ω^{T} is the weight and value are nonnegative, the threshold must be $0=r_0<r_1<\cdots<r_n<v_{\max}$. Observe **Figure 9**, and the same can be done by using the stop operator, this paper will not repeat it here.

3.1.4. Polynomial Model

Researchers have developed polynomial models based on the control accuracy of PEAs in various application scenarios. Although there is no universal formula,

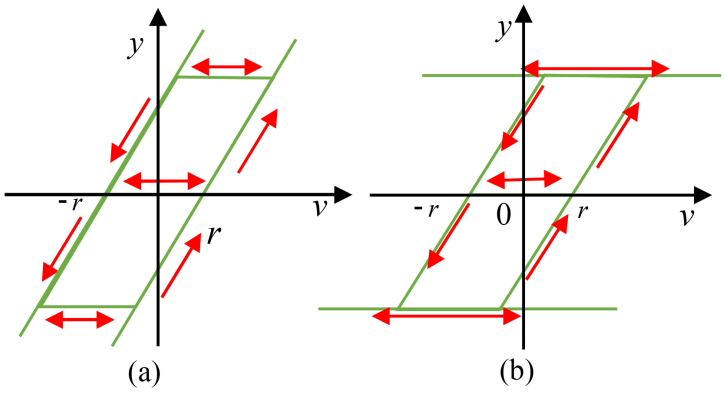

Figure 9. PI model basic operator. (a) The play operator [108]. (b) The stop operator [109].

hysteresis models using polynomials are all composed of linear functions to obtain polynomials [110] [111] [112] [113]. Examples of such polynomial models include.

$$\overline{y}_i = \beta_0 + \beta_1 x_i + \beta_2 x_i^2 + \cdots + \beta_p x_i^p + \varepsilon_i; i = 1, n \tag{7}$$

3.1.5. Bouc-Wen Model

Wen [114] proposed the Bouc-Wen model based on the differential equation proposed by Bouc [115] [116].

The Bouc-Wen model is expressed as follows.

$$F(x,t) = \alpha k x(t) + (1-\alpha) k z(t) \tag{8}$$

$$\dot{z} = A\dot{x} - \beta |\dot{x}| |z|^{n-1} z - \lambda \dot{x} |z|^n \tag{9}$$

where α is the ratio of the anterior and posterior terms and $\alpha \in (0,1)$, A, β and λ are dimensionless parameter; $F(x,t)$ is restoring force; x is the displacement; z is the output.

3.1.6. Duhem Model

Coleman and Hodgdon [117] refined Duhem's [118] differential equation, resulting in the Duhem model which is expressed mathematically as follows.

$$\frac{\mathrm{d}w}{\mathrm{d}t} = \alpha \left| \frac{\mathrm{d}v}{\mathrm{d}t} \right| \left[f(v) - w \right] + \frac{\mathrm{d}v}{\mathrm{d}t} g(v) \dot{f}(x) > g(x) > \alpha \mathrm{e}^{\alpha x} \int_x^\infty \left| \dot{f}(\varepsilon) - g(\varepsilon) \right| \mathrm{e}^{-\alpha\varepsilon} \mathrm{d}\varepsilon \tag{10}$$

where $f(v)$ and $g(v)$ are a given continuous function, The former is an odd function that increases monotonically and is piecewise smooth, and the latter is a piecewise smooth continuous even function. Both of them are bounded in their domain. $\dot{f}(x) > g(x) > \alpha \mathrm{e}^{\alpha x} \int_x^\infty \left| \dot{f}(\varepsilon) - g(\varepsilon) \right| \mathrm{e}^{-\alpha\varepsilon} \mathrm{d}\varepsilon$ is true for any $x > 0$. α is a constant, v is the input and w is the output.

3.1.7. Backlash-Like Model

Su *et al.* [119] proposed a dynamic hysteresis backlash model based on first-order differential equation. The expression of the Backlash-like model is as follows.

$$p(v(t))=\begin{cases} c(v(t)-B) & \dot{v}(t)>0, w(t)=c(v(t)-B) \\ c(v(t)+B) & \dot{v}(t)<0, w(t)=c(v(t)+B) \\ w(t\_) & \dot{v}(t)=0 \end{cases} \tag{11}$$

where $v(t)$ is the model input, $w(t)$ is the model output, $c>0$, $B>0$.

3.1.8. Dahl Model

Dahl [120] proposed the Dahl model based on friction phenomenon as follows [121].

$$\frac{\mathrm{d}F}{\mathrm{d}t}=\delta\left|1-\frac{F}{Fc}\mathrm{sgn}(\dot{x})\right|^{i}\mathrm{sgn}\left(1-\frac{F}{Fc}\mathrm{sgn}(\dot{x})\right) \tag{12}$$

where F is the static friction, Fc is the sliding friction, x is the output displacement. The slope of the force curve under $F=0$ is denoted by δ, and i denotes the different kinds of piezoelectric materials. Both δ and i should be set to 1 when researchers study the hysteresis behaviour of piezoelectric materials.

The Dahl model is as follows.

$$\frac{\mathrm{d}F}{\mathrm{d}t}=\frac{\mathrm{d}x}{\mathrm{d}t}-\frac{F}{Fc}\left|\frac{\mathrm{d}x}{\mathrm{d}t}\right| \tag{13}$$

$$\frac{\mathrm{d}^2x}{\mathrm{d}t^2}+\gamma\frac{\mathrm{d}x}{\mathrm{d}t}+k_nx=k_vx-k_iF \tag{14}$$

where v stands for the input voltage, and x stands for the output displacement. k_i and Fc determine the shape of the hysteresis loop. The remaining unknowns are model parameters that need to be identified. Because of the existence of differential equations in the Dahl model, the control method can be designed simply in the Dahl model [81] [122] [123].

3.2. Physics-Based Models

The physical model is based on materials science, thermodynamics, and physics theories. The generation of hysteresis is studied using the theories of electric domain turning, molecular polarization, ferroelectric, and parametric phase transitions. Physical-based models of hysteresis include Ikuta model, Maxwell model, and Jiles-Atherton model.

Among them, the most representative physical model is the ferromagnetic hysteresis model proposed by Jiles and Atherton [124] in 1986, and the reversible transition mechanism of ferromagnetic materials were analysed in detail. Subsequently, Smith proposed a domain wall model to describe the hysteresis of piezoelectric materials based on the Jiles and Atherton model [125] and published a work on hysteresis genesis and physical modelling of ferromagnetic materials in 2005 [83]. By studying the relationship between stress and strain of SMA materials, Ikuta *et al.* [84] proposed a mechanical model to describe the hysteresis of SMA.

3.2.1. Ikuta Model

The Ikuta model is a sublayer model [126] proposed by Ikuta *et al.* [127] for SMA.

As shown in Figure 10, the researchers found that the temperature-martensite fraction exhibits hysteresis loops during the heating and cooling of SMA materials. The Ikuta model uses an exponential function to fit the phase transition in the temperature change process. Equation (17) provides the phase fraction during heating. The phase fraction of SMA materials during heating is shown in Equation (20), and the cooling process is the same [128].

3.2.2. Maxwell Model

The Maxwell model is originally proposed by James C. Maxwell [130]. The hysteresis behaviour of the unloaded PEA can be simulated by an equivalent circuit consisting of n serially connected charge-saturated capacitors (CSC), as illustrated in Figure 11. Thus, the governing equation of a PEA is as follow.

$$\dot{q}(t)=\begin{cases}\dot{q}(t) & |q_i(t)|<Q_i\\ 0 & |q_i(t)|\geq Q_i\end{cases} \tag{15}$$

$$q(t)=C_i u_i(t) \tag{16}$$

$$u(t)=\sum_i^n u_i(t) \tag{17}$$

$$q(t)=Tx(t) \tag{18}$$

where q_i and u_i are the charge stored in the charge-saturated capacitor CSC_i and the voltage applied on it, C_i and Q_i are its capacitance and capability to store charge, x and q are the PEA's output displacement and the charge stored in it, and T is the electro-mechanical transfer ratio from effective displacement x to charge q.

3.2.3. Jiles-Atherton Model

Jiles and Atherton [124] present the ferromagnet hysteresis model in mathematical form based on the concept of domain wall motion. Chen *et al.* [131] found that the modified Jiles-Atherton model can simulate permanent magnets. The

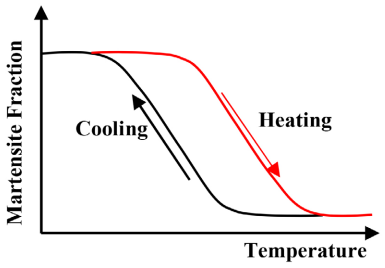

Figure 10. Hysteresis loop and transformation temperatures of an SMA material [129].

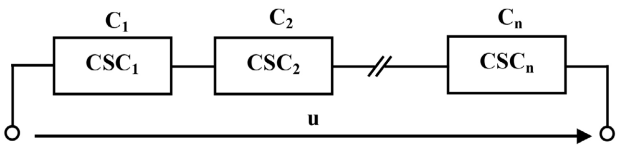

Figure 11. Equivalent circuit of unloaded PEA [130].

modified Jiles-Atherton model can accurately and stably describe the dynamic magnetization behaviour of magnetic particles [132]. Classical Jiles-Atherton model equations as follow [133].

$$M_{rev} = c\left(M_{an} - M_{irr}\right) \tag{19}$$

where M is magnetisation, M_{rev} is reversible and M_{irr} is irreversible components. M_{an} is an hysteretic magnetisation and based on the Langevin function they get the following.

$$M_{an} = M_s\left[\coth\left(\frac{H_e}{a} - \frac{a}{H_e}\right)\right] \tag{20}$$

With,

$$\frac{\mathrm{d}M_{irr}}{\mathrm{d}H_e} = \frac{M_{an} - M_{irr}}{k\delta} \tag{21}$$

where $H_e = H + \alpha M$ is the effective field experienced by the magnetic domains. The model parameters are M_s, a, α, c and k. δ is a directional parameter assuming the value +1 if $\mathrm{d}H/\mathrm{d}t > 0$, otherwise the value is −1. Jiles-Atherton model can be written as follow.

$$\frac{\mathrm{d}M}{\mathrm{d}H} = \frac{(1-c)\left(\mathrm{d}M_{irr}/\mathrm{d}H_e\right) + c\left(\mathrm{d}M_{an}/\mathrm{d}H_e\right)}{1 - \alpha(1-c)\left(\mathrm{d}M_{irr}/\mathrm{d}H_e\right) - \alpha c\left(\mathrm{d}M_{an}/\mathrm{d}H_e\right)} \tag{22}$$

3.3. Other Models

There are various models of PEAs, including the parabolic model, hyperbolic function model, exponential fitting model, and support vector machine model. This section presents the classical hysteresis model and associated concepts of PEAs. Accuracy requirements of precision control systems and hybrid models have become a new trend in the hysteresis modelling of PEAs [109] [134], and the specific content will be discussed in Section 4 of this paper.

3.3.1. Artificial Neural Network Models

Compared with other models, neural network models have the characteristics of self-learning, self-correction, and high-precision approximation and are widely used in nonlinear system identification and controller design [135]. Because the neural network model can only describe one-to-one mapping [136], and the piezoelectric transducer has multi-value properties and memory properties, the neural network model cannot be directly used to describe the hysteresis behaviour of the piezoelectric transducer. Generally, the composite algorithm combining neural networks and other methods describes the hysteresis nonlinearity [137]. In addition, Quondam-Antonio *et al.* [138] used neural networks to model the hysteresis behaviour-related characteristics and were able to reproduce the evolution of the magnetization process under arbitrary excitation waveforms.

3.3.2. Ellipse Fitting Model

Some scholars used elliptic curves to describe the hysteresis characteristics of

piezoelectric materials because the hysteresis loop is very similar to an ellipse. The hysteresis curve includes a rising and falling curve, similar to a part of an elliptic curve, so Zou *et al.* [139] use the polar elliptic curve method for modelling. The general equation of an ellipse is:

$$Ax^2 + Bxy + Cy^2 + Dx + Ey + F = 0 \tag{23}$$

Define $x' = x - x_0$, $y' = y - y_0$, Then the elliptic equation can be rewritten as.

$$A(x - x_0)^2 + B(x - x_0)(y - y_0) + C(y - y_0)^2 + f = 0 \tag{24}$$

So the solution is:

$$Ax'^2 + Bx'y' + Cy' + f = 0 \tag{25}$$

The standard equation is:

$$\frac{\tilde{x}^2}{a^2} + \frac{\tilde{y}^2}{b^2} = 1 \tag{26}$$

The relationship between $\tilde{x}$ and x' as follows.

$$\begin{cases} \tilde{x} = x'\cos\theta - y'\sin\theta \\ \tilde{y} = x'\sin\theta - y'\cos\theta \end{cases} \tag{27}$$

It can be obtained by combining Equations (25) and (26).

$$\frac{x'\cos\theta - y'\sin\theta}{a^2} + \frac{x'\sin\theta - y'\cos\theta}{b^2} \tag{28}$$

Each parameter in the equation is obtained by comparing Equation (12) with Equation (17).

$$\begin{cases} A = a^2\sin\theta + b^2\cos\theta \\ B = 2\left(a^2 + b^2\right)\sin\theta\cos\theta \\ C = a^2\cos^2\theta + b^2\sin^2\theta \\ D = -a^2b^2 \end{cases} \tag{29}$$

In this section, typical hysteresis models are briefly introduced and classified. To further investigate the hysteresis model, the hysteresis modelling based on the typical model and other hysteresis models are introduced in the following subsections.

4. Hysteresis Modelling for PEAs

As can be observed from the aforementioned, a series of actuators based on high-performance piezoelectric materials have emerged. However, the inherent hysteresis of these materials severely constrains their development in the field of high-precision control. To enhance accuracy and design PEAs with greater efficacy, this paper aims to further investigate hysteresis modelling. As illustrated in **Figure 12**, the hysteresis modelling of PEAs can be categorized into decoupling and coupling types based on overall and partial modelling approaches. The hysteresis model of a PEA as part of the PEA model is referred to as decoupling [140], while hysteresis modelling that does not consider external driver

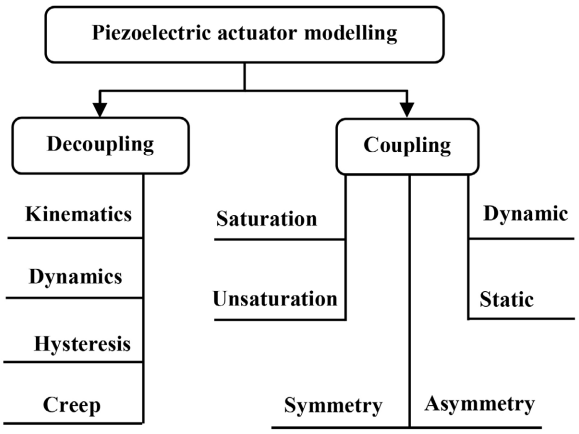

Figure 12. Categorization of hysteresis modelling approaches for PEAs.

environment is known as coupling [141] [142] [143]. During actual decoupling, the PEA is divided into several submodels based on practical situations. The Figure 12 serves only as a reference. Coupling hysteresis can be categorized into saturation and unsaturation [144], dynamic and static [145] [146], symmetric and asymmetric types [147] [148]. This section, we provide a brief review of contemporary hysteresis modelling techniques for PEAs, with a focus on the correlation model of the inverse hysteresis model. We also attempt to summarize the general steps involved in hysteresis modelling across various approaches.

4.1. Inverse of Hysteresis Modelling (IOHM)

Hysteresis compensation and control during the process of curve linearization modelling for PEAs' hysteresis characteristics can be found in reference [149] [150]. Table 1 illustrates the focus of this section on the solution method for IOHM, with references to recent literature. Key components of hysteresis modelling discussed in Table 1 include classical models, control methods, direct IOHM, direct IOHM and algorithms. The latest advancements in direct IOHM and indirect IOHM are also evaluated. Direct IOHM [151] [152] [153] [154], in contrast to indirect IOHM, can directly invert the voltage displacement curve to obtain the displacement voltage curve and solve the inverse hysteresis model without solving the hysteresis model first [155].

4.1.1. Direct IOHM

There are many cases where the direct IOHM is employed. In 2012, Guo *et al.* [164] utilized an enhanced PI model and aimed at the asymmetric inverse hysteresis effect and subsequently employed the adaptive particle swarm optimization (PSO) algorithm to solve the inverse hysteresis model of real-time control. In the same year, Qin *et al.* [151] found that rate-independent PI model inversion parsing is desirable They employed the inverse PI model as a feedforward controller for a piezoelectric actuated compliant mechanism, obtaining the inverse PI model directly from experimental data. This method avoids solving the inverse of the PI model and is also effective for the rate-dependent PI model. In

Table 1. Modelling and compensation methods for piezoelectric hysteresis.

References	Base model	Control method	Direct IOHM	Indirect IOHM	Algorithm
[156]	Modified PI	Feedforward	Negative	Existence	Error back-propagation algorithm.
[157]	Modified Bouc–Wen	Feedforward	Negative	Existence	Self-adaptive cooperative PSO algorithm.
[158]	Data separated by a PI	Feedforward	Negative	Existence	A novel differential evolution algorithm.
[159]	The hysteresis submodel	Feedforward	Existence	Negative	Radial basis function neural network.
[160]	Temperature-dependent asymmetric PI	Feedback	Negative	Existence	Parameter estimation algorithm.
[85]	Rate-dependent asymmetric hysteresis PI	Robust adaptive controller	Negative	Negative	Improved genetic algorithm.
[161]	Least-squares support-vector machines based on nonlinear auto-regressive exogenous	Incremental PID controller	Negative	Existence	PSO algorithm. Least-squares support-vector machines regression algorithm.
[162]	Back propagation neural network	PID	Negative	Existence	Adaptive particle swarm algorithm.
[163]	Hybrid static hysteresis	Feedforward	Negative	Existence	PSO algorithm.

2017, Ko *et al.* [165] proposed a generalized PI model-based inverse feedforward compensation approach for addressing asymmetric hysteresis nonlinearity. In 2020, Lallart *et al.* [166] proposed a system-level inverse method to simulate the quasi-static hysteresis of a PEA and demonstrated it on a piezoelectric transducer. This approach for solving the direct inverse model of the direct hysteresis model is well-suited for implementation in embedded control systems. In 2021, Qin *et al.* [154] achieved high-precision hysteresis compensation over a more comprehensive frequency range. They used the direct inverse modelling method to build a multilayer feedforward neural network inverse model as a feedforward lag compensator. In the same period, Zhang *et al.* [167] aimed to enhance the precision of piezoelectric fast steering mirror's swing. They proposed the Hammerstein dynamic inverse hysteresis model for PEAs. In addition to this, the authors employed the generalized Bouc-Wen inverse model to characterize static nonlinearity and utilized the autoregressive exogenous model to capture rate dependence. The hybrid model parameters are then identified through employment of the adaptive PSO algorithm. This method avoids the complex inverse process of the Bouc-Wen model and is suitable for rate-dependent and asymmetric hysteresis behaviour. In 2022, Nguyen Ngoc Son *et al.* [168] proposed neuroevolutionary adaptive sliding mode control for solving piezoelectric ceramic actuators' nonlinearity. They utilized the neuroevolution model to identify the inverse hysteresis model of piezoelectric ceramic actuators, and employed both

differential evolution algorithm and Jaya algorithm for global and local optimization respectively. In the same period, Nie *et al.* [85] proposed a rate-dependent asymmetric hysteresis model based on the PI model. They introduced the dynamic envelope function year into the Play operator, which has a simple structure and few parameters.

4.1.2. Indirect IOHM

In 2006, to solve the problem that there is no inverse of the PI operator when the PI model is not positive definite, Tan *et al.* [169] extended the PI operator and then calculated the inverse hysteresis PI model for feedforward controller. As early as 2009, Yang *et al.* [170] adopted Preisach and BP neural networks and used a linear interpolation algorithm. In 2016, the identification of at least ten parameters is required for the PI model, so Gan *et al.* [171] combined quadratic polynomials and linear equations to identify only four parameters and solve the PEA hysteresis model. Finally, the IOHM is obtained and applied to real-time hybrid control. In 2018, Janaideh *et al.* [172] proposed a solution to address the saturation and asymmetric energy phenomena observed in PEA under high-frequency excitation and numerous inputs. With the rate-dependent PI model and a dead-zone operator as feedforward compensator, an inverse model for real-time compensation is established to effectively suppress asymmetric nonlinear hysteresis. In 2019, Tao *et al.* [173] order to solve the problem that the nano-positioning platform's positioning accuracy is subject to hysteresis effects. The hysteresis is modeled using a Gaussian process, and the parameters are determined through the integration of a differential evolution algorithm and Bayesian inference. The outputs based on the Gaussian process hysteresis model are then interleaved to obtain the inverse model as a feedforward compensator. This method is suitable for nonlinear, memory, and rate-dependent. hysteresis modelling. In 2020, Janaideh *et al.* [174] to mitigate the impact of temperature on the precise positioning of piezoelectric tube actuators. The simultaneous modelling of hysteresis nonlinearity and temperature effects is undertaken. Two different temperature-dependent Prandtl-Ishlinskii models are proposed, which are solved by MATLAB-Simulink and Grey Wolf optimization algorithms, respectively. The inverse model of the temperature-dependent Prandtl-Ishlinskii model is derived and utilized as a feedforward controller to compensate for the hysteresis nonlinearity exhibited by the piezoelectric tubular actuator. To improve the classical Preisach model, The dynamic hysteresis model has been presented by Chen *et al.* [145]. It is based on the classical Preisach model, and the dynamic term is introduced and solved numerically. The dynamic inverse model is ultimately implemented as the feedforward controller. In 2020, to address the limitation of the PI model in describing asymmetric hysteresis, Wang *et al.* [175] proposed the polynomial-modified Prandtl-Ishlinskii (PMPI) model that can describe both asymmetric and symmetric hysteresis. They used a modified-play operator and memoryless polynomial to form the PMPI model. They used a differential evolution algorithm and a simplex algorithm to identify the parameters

of the PMPI model. Global and local optima are then obtained to search the hysteresis model in the design into an inverse model feedforward compensator. In 2021, The piezoelectric sensor-actuator was designed by Shan *et al.* [176] and applied to a micro-high precision integrated system. They proposed nonlinear and inverse models based on dynamic hysteresis using quasi-static models and linear transfer functions. Based on classical hysteresis modelling, it is typically necessary to optimize the algorithm within the model in order to enhance its modelling accuracy. Hysteresis modelling based on the hybrid model is usually divided into direct IOHM and indirect IOHM. The former solves the inverse model of the hybrid model as a feedforward controller, followed by the series hysteresis model. Its characteristic is that the choice of the hysteresis model must be able to solve the inverse analysis, the inverse hysteresis accuracy depends on the hysteresis model accuracy, and the structure is simple. The latter is to solve the direct inverse model using the known output input data as a feedforward compensator and then concatenate the hysteresis models. Its characteristics are that it can be modelled based on irreversible hysteresis, the direct inverse hysteresis model is not associated with the hysteresis model, and it has many parameters. In the last decade, due to the diversity of ideas for PEA hysteresis modelling.

4.2. Hysteresis Modelling Steps

The hysteresis modelling of a PEA, as illustrated in **Figure 13**, comprises three steps: model determination, parameter estimation, and output hysteresis loop. The aforementioned component can serve as the precursor for hysteresis compensation design, enabling the creation of a well-designed compensator that can be integrated with the control system to achieve linear PEA control.

4.2.1. Specify a Category of Models

The hysteresis models in the current literature include not only single and multiple models based on classical approaches [177] [178], but also those based on

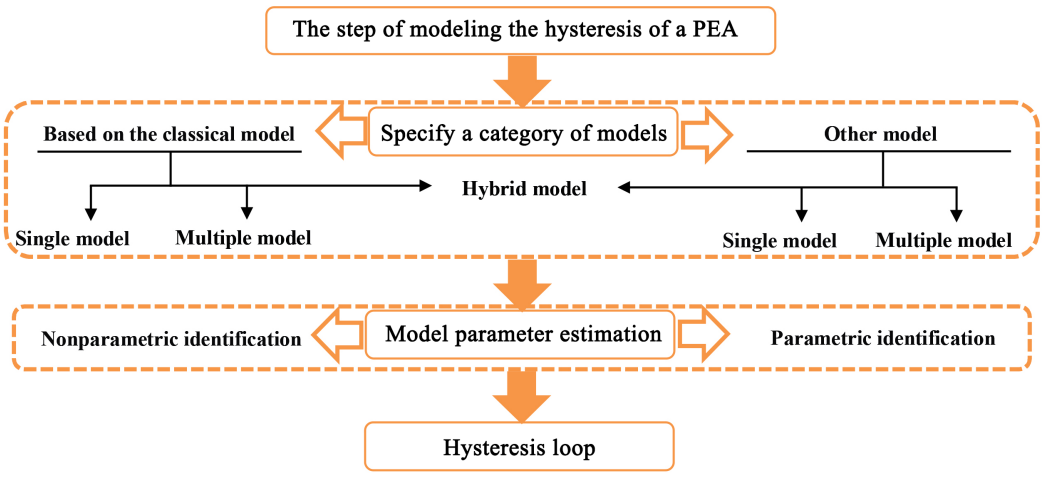

Figure 13. The step of modelling the hysteresis.

the other models [179] [180]. There are also hybrid models that combine the classical models with the other models [181].

4.2.2. Model Parameter Estimation

The model parameters can be estimated using both nonparametric and parametric identification methods. Nonparametric identification refers to designing the recognizer to mimic the behaviour of the real system in order to minimize error, while parameter identification involves estimation through optimization tools [109]. The original input and output data of the PEA serve as known variables in solving for the parameters using the aforementioned method.

4.2.3. Hysteresis Loop

The original input data is fed into the hysteresis model to obtain the output, which is then compared with the original data output to determine modelling accuracy. At this point, hysteresis modelling is completed. In addition to the improvement of hardware equipment accuracy, the following methods are commonly employed in hysteresis modelling to enhance its accuracy.

1) Design an enhanced classical model by refining the fundamental computational units within the classical models.

2) Develop improved algorithms for identifying unknown parameters in the classical models.

3) Explore hybridization of the classical models with the other model using varying weights.

5. Conclusion

Piezoelectric materials have found extensive applications in various industries. However, the issues of hysteresis and nonlinear control in achieving high precision for piezoelectric materials require resolution. This paper introduces the characteristics of PEAs and summarizes the typical applications and hysteresis modelling models of PEAs. Then the hysteresis modelling steps of the PEAs are proposed. The critical points of PEAs hysteresis modelling are summarized, including the selection of a classical model, parameter identification algorithm and hysteresis compensation method. It is suggested that algorithm optimization and hybrid hysteresis model will be the preferred options for high-precision hysteresis modelling of PEAs in the future.

Conflicts of Interest

The author declares no conflicts of interest.

References

[1] Sezer, N. and Koç, M. (2021) A Comprehensive Review on the State-of-the-Art of Piezoelectric Energy Harvesting. *Nano Energy*, **80**, Article ID: 105567. https://doi.org/10.1016/j.nanoen.2020.105567

[2] Wu, Y., Ma, Y., Zheng, H. and Ramakrishna, S. (2021) Piezoelectric Materials for Flexible and Wearable Electronics: A Review. *Materials & Design*, **211**, Article ID:

110164. https://doi.org/10.1016/j.matdes.2021.110164

[3] Ding, B., Zhao, J. and Li, Y. (2021) Design of A Spatial Constant-Force End-Effector for Polishing/Deburring Operations. *The International Journal of Advanced Manufacturing Technology*, **116**, 3507-3515. https://doi.org/10.1007/s00170-021-07579-1

[4] Jin, H., *et al.* (2022) Review on Piezoelectric Actuators Based on High Performance Piezoelectric Materials. *IEEE Transactions on Ultrasonics, Ferroelectrics, and Frequency Control*, **69**, 3057-3069. https://doi.org/10.1109/TUFFC.2022.3175853

[5] Xing, J., Ning, C., Liu, Y. and Howard, I. (2022) Piezoelectric Inertial Robot for Operating in Small Pipelines Based on Stick-Slip Mechanism: Modeling and Experiment. *Frontiers of Mechanical Engineering*, **17**, Article No. 41. https://doi.org/10.1007/s11465-022-0697-z

[6] Curie, J. and Curie, P. (1880) Développement par compression de l'électricité polaire dans les cristaux hémièdres à faces inclinées. *Bulletin de minéralogie*, **3**, 90-93. https://doi.org/10.3406/bulmi.1880.1564

[7] Tian, X., Liu, Y., Deng, J., Wang, L. and Chen, W. (2020) A Review on Piezoelectric Ultrasonic Motors for the Past Decade: Classification, Operating Principle, Performance, and Future Work Perspectives. *Sensors and Actuators A*: *Physical*, **306**, Article ID: 111971. https://doi.org/10.1016/j.sna.2020.111971

[8] Safaei, M., Sodano, H.A. and Anton, S.R. (2019) A Review of Energy Harvesting Using Piezoelectric Materials: State-of-the-Art a Decade Later (2008-2018). *Smart Materials and Structures*, **28**, Article ID: 113001. https://doi.org/10.1088/1361-665X/ab36e4

[9] Aabid, A., *et al.* (2021) A Systematic Review of Piezoelectric Materials and Energy Harvesters for Industrial Applications. *Sensors*, **21**, Article No. 4145. https://doi.org/10.3390/s21124145

[10] Yang, Z., Zhou, S., Zu, J. and Inman, D. (2018) High-Performance Piezoelectric Energy Harvesters and Their Applications. *Joule*, **2**, 642-697. https://doi.org/10.1016/j.joule.2018.03.011

[11] Le, A.T., Ahmadipour, M. and Pung, S.-Y. (2020) A Review on ZnO-Based Piezoelectric Nanogenerators: Synthesis, Characterization Techniques, Performance Enhancement and Applications. *Journal of Alloys and Compounds*, **844**, Article ID: 156172. https://doi.org/10.1016/j.jallcom.2020.156172

[12] Soin, N., *et al.* (2016) High Performance Triboelectric Nanogenerators Based on Phase-Inversion Piezoelectric Membranes of Poly (Vinylidene Fluoride)-Zinc Stannate (PVDF-ZnSnO3) and Polyamide-6 (PA6). *Nano Energy*, **30**, 470-480. https://doi.org/10.1016/j.nanoen.2016.10.040

[13] Sarker, M.R., Julai, S., Sabri, M.F.M., Said, S.M., Islam, M.M. and Tahir, M. (2019) Review of Piezoelectric Energy Harvesting System and Application of Optimization Techniques to Enhance the Performance of the Harvesting System. *Sensors and Actuators A*: *Physical*, **300**, Article ID: 111634. https://doi.org/10.1016/j.sna.2019.111634

[14] Lu, C., *et al.* (2022) Wind Energy Harvester Using Piezoelectric Materials. *Review of Scientific Instruments*, **93**, Article ID: 031502. https://doi.org/10.1063/5.0065462

[15] Fakhri, P., *et al.* (2019) Flexible Hybrid Structure Piezoelectric Nanogenerator Based on ZnO nanorod/PVDF Nanofibers with Improved Output. *RSC Advances*, **9**, 10117-10123. https://doi.org/10.1039/C8RA10315A

[16] Deng, W., *et al.* (2019) Cowpea-Structured PVDF/ZnO Nanofibers Based Flexible Self-Powered Piezoelectric Bending Motion Sensor towards Remote Control of Gestures. *Nano Energy*, **55**, 516-525. https://doi.org/10.1016/j.nanoen.2018.10.049

[17] Singh, A., Monga, S., Sharma, N., Sreenivas, K. and Katiyar, R.S. (2022) Ferroelectric, Piezoelectric Mechanism and Applications. *Journal of Asian Ceramic Societies*, **10**, 275-291. https://doi.org/10.1080/21870764.2022.2075618

[18] Pop, F., Herrera, B. and Rinaldi, M. (2022) Lithium Niobate Piezoelectric Micromachined Ultrasonic Transducers for High Data-Rate Intrabody Communication. *Nature Communications*, **13**, Article No. 1782. https://doi.org/10.1038/s41467-022-29355-9

[19] Chen, W., Jia, W., Xiao, Y., Feng, Z. and Wu, G. (2021) A Temperature-Stable and Low Impedance Piezoelectric MEMS Resonator for Drop-In Replacement of Quartz Crystals. *IEEE Electron Device Letters*, **42**, 1382-1385. https://doi.org/10.1109/LED.2021.3094319

[20] Pulskamp, J.S., *et al.* (2012) Piezoelectric PZT MEMS Technologies for Small-Scale Robotics and RF Applications. *MRS Bulletin*, **37**, 1062-1070. https://doi.org/10.1557/mrs.2012.269

[21] Wang, P., *et al.* (2021) Ultrasmall Barium Titanate Nanoparticles for Highly Efficient Hypoxic Tumor Therapy via Ultrasound Triggered Piezocatalysis and Water Splitting. *ACS Nano*, **15**, 11326-11340. https://doi.org/10.1021/acsnano.1c00616

[22] Tian, J., Jiang, F., Zeng, Q., PourhosseiniAsl, M., Han, C. and Ren, K. (2023) Biocompatible Piezoelectric Polymer Poly (Lactic Acid)-Based Stethoscope for Wearable Health Monitoring Devices. *IEEE Sensors Journal*, **23**, 6264-6271. https://doi.org/10.1109/JSEN.2023.3240120

[23] Choi, N., *et al.* (2022) Fabrication and Simulation of a Piezoelectric PIN-PMN-PT Thin Film for Ultrahigh-Frequency Ultrasonic Transducers. *Sensors and Actuators A*: *Physical*, **347**, Article ID: 113936. https://doi.org/10.1016/j.sna.2022.113936

[24] Li, Z., *et al.* (2022) High-Frequency Self-Focusing Ultrasonic Transducer with Piezoelectric Metamaterial. *IEEE Electron Device Letters*, **43**, 946-949. https://doi.org/10.1109/LED.2022.3170613

[25] Guo, S., Duan, X., Xie, M., Aw, K.C. and Xue, Q. (2020) Composites, Fabrication and Application of Polyvinylidene Fluoride for Flexible Electromechanical Devices: A Review. *Micromachines*, **11**, Article No. 1076. https://doi.org/10.3390/mi11121076

[26] Yamashita, Y., Karaki, T., Lee, H.-Y., Wan, H., Kim, H.-P. and Jiang, X. (2022) A Review of Lead Perovskite Piezoelectric Single Crystals and Their Medical Transducers Application. *IEEE Transactions on Ultrasonics*, *Ferroelectrics*, *and Frequency Control*, **69**, 3048-3056. https://doi.org/10.1109/TUFFC.2022.3160526

[27] Tian, F., Liu, Y., Ma, R., Li, F., Xu, Z. and Yang, Y. (2021) Properties of PMN-PT Single Crystal Piezoelectric Material and Its Application in Underwater Acoustic Transducer. *Applied Acoustics*, **175**, Article ID: 107827. https://doi.org/10.1016/j.apacoust.2020.107827

[28] Wang, X., Huan, Y., Ji, S., Zhu, Y., Wei, T. and Cheng, Z. (2022) Ultra-High Piezoelectric Performance by Rational Tuning of Heterovalent-Ion Doping in Lead-Free Piezoelectric Ceramics. *Nano Energy*, **101**, Article ID: 107580. https://doi.org/10.1016/j.nanoen.2022.107580

[29] Yin, J., Chen, S., Wong, V.-K. and Yao, K. (2022)Thermal Sprayed Lead-Free Piezoelectric Ceramic Coatings for Ultrasonic Structural Health Monitoring. *IEEE Transactions on Ultrasonics*, *Ferroelectrics*, *and Frequency Control*, **69**, 3070-3080. https://doi.org/10.1109/TUFFC.2022.3176488

[30] Smith, M. and Kar-Narayan, S. (2022) Piezoelectric Polymers: Theory, Challenges and Opportunities. *International Materials Reviews*, **67**, 65-88.

https://doi.org/10.1080/09506608.2021.1915935

[31] Habib, M., Lantgios, I. and Hornbostel, K. (2022) A Review of Ceramic, Polymer and Composite Piezoelectric Materials. *Journal of Physics D*: *Applied Physics*, **55**, Article ID: 423002. https://doi.org/10.1088/1361-6463/ac8687

[32] Dong, K., Peng, X. and Wang, Z.L. (2020) Fiber/Fabric-Based Piezoelectric and Triboelectric Nanogenerators for Flexible/Stretchable and Wearable Electronics and Artificial Intelligence. *Advanced Materials*, **32**, Article ID: 1902549. https://doi.org/10.1002/adma.201902549

[33] Liu, L., *et al.* (2020) Nanowrinkle-Patterned Flexible Woven Triboelectric Nanogenerator toward Self-Powered Wearable Electronics. *Nano Energy*, **73**, Article ID: 104797. https://doi.org/10.1016/j.nanoen.2020.104797

[34] Wang, J., *et al.* (2020) Enhancement of Low-Speed Piezoelectric Wind Energy Harvesting by Bluff Body Shapes: Spindle-Like and Butterfly-Like Cross-Sections. *Aerospace Science and Technology*, **103**, Article ID: 105898. https://doi.org/10.1016/j.ast.2020.105898

[35] Edison, T.A. (1888) The Perfected Phonograph. *The North American Review*, **146**, 641-650.

[36] Rashid, A., Zubair, U., Ashraf, M., Javid, A., Abid, H.A. and Akram, S. (2023) Flexible Piezoelectric Coatings on Textiles for Energy Harvesting and Autonomous Sensing Applications: A Review. *Journal of Coatings Technology and Research*, **20**, 141-172. https://doi.org/10.1007/s11998-022-00690-2

[37] Palmer, S., *et al.* (2022) High Bandwidth Frequency Modulation of an External Cavity Diode Laser Using an Intracavity Lithium Niobate Electro-Optic Modulator as Output Coupler. *APL Photonics*, **7**, Article ID: 086106. https://doi.org/10.1063/5.0097880

[38] Xu, L., Liu, N., Zhou, S., Zhang, L. and Li, J. (2020) Dual-Spectroscopy Technique Based on Quartz Crystal Tuning Fork Detector. *Sensors and Actuators A*: *Physical*, **304**, Article ID: 111873. https://doi.org/10.1016/j.sna.2020.111873

[39] Choi, J., *et al.* (2017) Thin-Film Piezoelectric and High-Aspect Ratio Polymer Leg Mechanisms for Millimeter-Scale Robotics. *International Journal of Intelligent Robotics and Applications*, **1**, 180-194. https://doi.org/10.1007/s41315-017-0017-7

[40] Ling, J., Wang, K., Wang, Z., Huang, H. and Zhang, G. (2020) Enhanced Piezoelectric-Induced Catalysis of $SrTiO_3$ Nanocrystal with Well-Defined Facets under Ultrasonic Vibration. *Ultrasonics Sonochemistry*, **61**, Article ID: 104819. https://doi.org/10.1016/j.ultsonch.2019.104819

[41] Chen, D., *et al.* (2021) Recent Development and Perspectives of Optimization Design Methods for Piezoelectric Ultrasonic Transducers. *Micromachines*, **12**, Article No. 779. https://doi.org/10.3390/mi12070779

[42] Wan, L.F., Nishimatsu, T. and Beckman, S. (2012) The Structural, Dielectric, Elastic, and Piezoelectric Properties of $KNbO_3$ from First-Principles Methods. *Journal of Applied Physics*, **111**, Article ID: 104107. https://doi.org/10.1063/1.4712052

[43] Dong, L., *et al.* (2020) Cardiac Energy Harvesting and Sensing Based on Piezoelectric and Triboelectric Designs. *Nano Energy*, **76**, Article ID: 105076. https://doi.org/10.1016/j.nanoen.2020.105076

[44] Sakamiya, M., Fang, Y., Mo, X., Shen, J. and Zhang, T. (2020) A Heart-on-a-Chip Platform for Online Monitoring of Contractile Behavior via Digital Image Processing and Piezoelectric Sensing Technique. *Medical Engineering & Physics*, **75**, 36-44. https://doi.org/10.1016/j.medengphy.2019.10.001

[45] Park, S., *et al.* (2018) PVDF-Based Piezoelectric Microphone for Sound Detection

Inside the Cochlea: Toward Totally Implantable Cochlear Implants. *Trends in Hearing*, **22**, Article ID: 2331216518774450.
https://doi.org/10.1177/2331216518774450

[46] Guo, Z., *et al.* (2020) Self-Powered Sound Detection and Recognition Sensors Based on Flexible Polyvinylidene Fluoride-Trifluoroethylene Films Enhanced by *in-Situ* Polarization. *Sensors and Actuators A*: *Physical*, **306**, Article ID: 111970.
https://doi.org/10.1016/j.sna.2020.111970

[47] Yang, Z., Chen, C., Chen, W., Chen, H. and Liu, Z. (2022) Improved Sliding Mode Dynamic Matrix Control Strategy: Application on Spindle Loading and Precision Measuring Device Based on Piezoelectric Actuator. *Mechanical Systems and Signal Processing*, **167**, Article ID: 108543. https://doi.org/10.1016/j.ymssp.2021.108543

[48] Al Janaideh, M. and Rakotondrabe, M. (2021) Precision Motion Control of a Piezoelectric Cantilever Positioning System with Rate-Dependent Hysteresis Nonlinearities. *Nonlinear Dynamics*, **104**, 3385-3405.
https://doi.org/10.1007/s11071-021-06460-w

[49] Zhang, S.-Q., Zhao, G.-Z., Rao, M.N., Schmidt, R. and Yu, Y.-J. (2019) A Review on Modeling Techniques of Piezoelectric Integrated Plates and Shells. *Journal of Intelligent Material Systems and Structures*, **30**, 1133-1147.
https://doi.org/10.1177/1045389X19836169

[50] Du, S., Jia, Y., Zhao, C., Amaratunga, G.A. and Seshia, A.A. (2019) A Nail-Size Piezoelectric Energy Harvesting System Integrating a MEMS Transducer and a CMOS SSHI Circuit. *IEEE Sensors Journal*, **20**, 277-285.
https://doi.org/10.1109/JSEN.2019.2941180

[51] Ding, Y., Cai, Y. and Li, Y. (2022) Continuously Adjustable Micro Valve Based on a Piezoelectric Actuator for High-Precision Flow Rate Control. *Electronics*, **11**, Article No. 1689. https://doi.org/10.3390/electronics11111689

[52] Mohith, S., Upadhya, A.R., Navin, K.P., Kulkarni, S. and Rao, M. (2020) Recent Trends in Piezoelectric Actuators for Precision Motion and Their Applications: A Review. *Smart Materials and Structures*, **30**, Article ID: 013002.
https://doi.org/10.1088/1361-665X/abc6b9

[53] Kim, B., Washington, G.N. and Yoon, H.-S. (2014) Control and Hysteresis Reduction in Prestressed Curved Unimorph Actuators Using Model Predictive Control. *Journal of Intelligent Material Systems and Structures*, **25**, 290-307.
https://doi.org/10.1177/1045389X13493353

[54] Haller, D., *et al.* (2011) Piezo-Polymer-Composite Unimorph Actuators for Active Cancellation of Flow Instabilities across Airfoils. *Journal of Intelligent Material Systems and Structures*, **22**, 461-474. https://doi.org/10.1177/1045389X10395794

[55] Ovezea, D., *et al.* (2022) Exeprimental Testing of a Tremor Compensation System with Bimorph Piezoceramic Actuators Using Optical Methods. *International Journal of Mechatronics and Applied Mechanics*, No. 11, 31-41.

[56] van den Ende, D., Bos, B. and Groen, W. (2009) Non-Linear Electromechanical Behaviour of Piezoelectric Bimorph Actuators: Influence on Performance and Lifetime. *Journal of Electroceramics*, **22**, 185-191.
https://doi.org/10.1007/s10832-008-9459-5

[57] Habineza, D., Rakotondrabe, M. and Gorrec, Y.L. (2016) Characterization, Modeling and H_∞ Control of n-DOF Piezoelectric Actuators: Application to a 3-DOF Precise Positioner. *Asian Journal of Control*, **18**, 1239-1258.
https://doi.org/10.1002/asjc.1224

[58] Kuiper, S. and Schitter, G. (2010) Active Damping of a Piezoelectric Tube Scanner

Using Self-Sensing Piezo Actuation. *Mechatronics*, **20**, 656-665. https://doi.org/10.1016/j.mechatronics.2010.07.003

[59] Li, W., Yang, Z., Li, K. and Wang, W. (2021) Hybrid Feedback PID-FxLMS Algorithm for Active Vibration Control of Cantilever Beam with Piezoelectric Stack Actuator. *Journal of Sound and Vibration*, **509**, Article ID: 116243. https://doi.org/10.1016/j.jsv.2021.116243

[60] Wang, S., Rong, W., Wang, L., Xie, H., Sun, L. and Mills, J.K. (2019) A Survey of Piezoelectric Actuators with Long Working Stroke in Recent Years: Classifications, Principles, Connections and Distinctions. *Mechanical Systems and Signal Processing*, **123**, 591-605. https://doi.org/10.1016/j.ymssp.2019.01.033

[61] Koyuncu, A. (2022) Design, Modelling and Analysis of a Novel Implantable bone Conduction Hearing Aid with a Piezoelectric Actuator. Middle East Technical University, Ankara.

[62] Ding, B., Li, X. and Li, Y. (2022) Configuration Design and Experimental Verification of a Variable Constant-Force Compliant Mechanism. *Robotica*, **40**, 3463-3475. https://doi.org/10.1017/S0263574722000340

[63] Sun, W., *et al*. (2022) An Impact Inertial Piezoelectric Actuator Designed by Means of the Asymmetric Friction. *IEEE Transactions on Industrial Electronics*, **70**, 699-708. https://doi.org/10.1109/TIE.2022.3153807

[64] Ding, B., Yang, Z.-X., Zhang, G. and Xiao, X. (2017) Optimum Design and Analysis of Flexure Based Mechanism for Non-Circular Diamond Turning Operation. *Advances in Mechanical Engineering*, **9**, Article ID: 1687814017743353. https://doi.org/10.1177/1687814017743353

[65] Liu, Y., Deng, J. and Su, Q. (2018) Review on Multi-Degree-of-Freedom Piezoelectric Motion Stage. *IEEE Access*, **6**, 59986-60004. https://doi.org/10.1109/ACCESS.2018.2875940

[66] Sun, X., Chen, W., Zhang, J., Zhou, R. and Chen, W. (2015) A Novel Piezo-Driven Linear-Rotary Inchworm Actuator. *Sensors and Actuators A*: *Physical*, **224**, 78-86. https://doi.org/10.1016/j.sna.2015.01.024

[67] Ding, B., Li, Y., Xiao, X., Tang, Y. and Li, B. (2017) Design and Analysis of a 3-DOF Planar Micromanipulation Stage with Large Rotational Displacement for Micromanipulation System. *Mechanical Sciences*, **18**, 117-126. https://doi.org/10.5194/ms-8-117-2017

[68] Wang, L., Chen, W., Liu, J., Deng, J. and Liu, Y. (2019) A Review of Recent Studies on Non-Resonant Piezoelectric Actuators. *Mechanical Systems and Signal Processing*, **133**, Article ID: 106254. https://doi.org/10.1016/j.ymssp.2019.106254

[69] Ding, B., Li, X. and Li, Y. (2021) FEA-Based Optimization and Experimental Verification of a Typical Flexure-Based Constant Force Module. *Sensors and Actuators A*: *Physical*, **332**, Article ID: 113083. https://doi.org/10.1016/j.sna.2021.113083

[70] Li, J., Huang, H. and Morita, T. (2019) Stepping Piezoelectric Actuators with Large Working Stroke for Nano-Positioning Systems: A Review. *Sensors and Actuators A*: *Physical*, **292**, 39-51. https://doi.org/10.1016/j.sna.2019.04.006

[71] Yang, C., Wang, Y. and Fan, W. (2022) Long Stroke Design of Piezoelectric Walking Actuator for Wafer Probe Station. *Micromachines*, **13**, Article No. 412. https://doi.org/10.3390/mi13030412

[72] Qi, H.Y. (2019) Influence of Waveform Symmetry on Output Performance of Piezoelectric Inertia Actuator Controlled by Composite Method. *IOP Conference Series*: *Materials Science and Engineering*, **565**, Article ID: 012014. https://doi.org/10.1088/1757-899X/565/1/012014

[73] Shao, Y., Xu, M., Shao, S. and Song, S. (2020) Effective Dynamical Model for Piezoelectric Stick-Slip Actuators in Bi-Directional Motion. *Mechanical Systems and Signal Processing*, **145**, Article ID: 106964. https://doi.org/10.1016/j.ymssp.2020.106964

[74] Wang, X., Zhu, L. and Huang, H. (2020) A Dynamic Model of Stick-Slip Piezoelectric Actuators Considering the Deformation of Overall System. *IEEE Transactions on Industrial Electronics*, **68**, 11266-11275. https://doi.org/10.1109/TIE.2020.3032922

[75] Bai, D., Li, Y., Quan, Q., Tang, D. and Deng, Z. (2023) Development of a Rotary-Percussive Ultrasonic Drill Using a Bolt-Clamped Type Piezoelectric Actuator. *Advances in Space Research*, **71**, 5360-5368. https://doi.org/10.1016/j.asr.2023.02.008

[76] Suryawanshi, P. and Arunkumar, G. (2022) A Review on Design and Development of Multi Degree of Freedom Compliant Mechanism. *AIP Conference Proceedings*, **2460**, Article ID: 080005. https://doi.org/10.1063/5.0095660

[77] Wei, F., Wang, X., Dong, J., Guo, K. and Sui, Y. (2023) Development of a Three-Degree-of-Freedom Piezoelectric Actuator. *Review of Scientific Instruments*, **94**, Article ID: 025001. https://doi.org/10.1063/5.0114030

[78] Čeponis, A., Jūrėnas, V. and Mažeika, D. (2022) Development of 5-DOF Piezoelectric Actuator for Planar—Angular Positioning. *Applied Sciences*, **12**, Article No. 1033. https://doi.org/10.3390/app12031033

[79] Gao, X., *et al*. (2020) Piezoelectric Actuators and Motors: Materials, Designs, and Applications. *Advanced Materials Technologies*, **5**, Article ID: 1900716. https://doi.org/10.1002/admt.201900716

[80] Wang, G., Yao, X., Cui, J., Yan, Y., Dai, J. and Zhao, W. (2020) A Novel Piezoelectric Hysteresis Modeling Method Combining LSTM and NARX Neural Networks. *Modern Physics Letters B*, **34**, Article ID: 2050306. https://doi.org/10.1142/S0217984920503066

[81] Gan, J. and Zhang, X. (2019) A Review of Nonlinear Hysteresis Modeling and Control of Piezoelectric Actuators. *AIP Advances*, **9**, Article ID: 040702. https://doi.org/10.1063/1.5093000

[82] Mayergoyz, I.D. (2003) Mathematical Models of Hysteresis and Their Applications. Academic Press, Cambridge, Massachusetts.

[83] Smith, R.C. (2005) Smart Material Systems: Model Development. In: *Frontiers in Applied Mathematics*, Society for Industrial and Applied Mathematics, Philadelphia. https://doi.org/10.1137/1.9780898717471

[84] Ding, B.X. and Li, Y.M. (2018) Hysteresis Compensation and Sliding Mode Control with Perturbation Estimation for Piezoelectric Actuators. *Micromachines*, **9**, Article No. 241. https://doi.org/10.3390/mi9050241

[85] Nie, L., Luo, Y., Gao, W. and Zhou, M. (2022) Rate-Dependent Asymmetric Hysteresis Modeling and Robust Adaptive Trajectory Tracking for Piezoelectric Micropositioning Stages. *Nonlinear Dynamics*, **108**, 2023-2043. https://doi.org/10.1007/s11071-022-07324-7

[86] Xu, M., Zhang, J.-Q., Rong, C. and Ni, J. (2020) Multislope PI Modeling and Feedforward Compensation for Piezoelectric Beam. *Mathematical Problems in Engineering*, **2020**, Article ID: 6404971. https://doi.org/10.1155/2020/6404971

[87] Preisach, F. (1935) Über die magnetische Nachwirkung. *Zeitschrift für Physik*, **94**, 277-302. https://doi.org/10.1007/BF01349418

[88] Krasnosel'skii, M.A., and Pokrovskii, A.V. (2012) Systems with Hysteresis. Springer

Science & Business Media, Berlin.

[89] Mayergoyz, I. (1986) Mathematical Models of Hysteresis. *IEEE Transactions on Magnetics*, **22**, 603-608. https://doi.org/10.1109/TMAG.1986.1064347

[90] Wawrzała, P. (2013) Application of a Preisach Hysteresis Model to the Evaluation of PMN-PT Ceramics Properties. *Archives of Metallurgy and Materials*, **58**, 1347-1350. https://doi.org/10.2478/amm-2013-0172

[91] Yang, L., Ding, B.X., Liao, W.H. and Li, Y.M. (2022) Identification of Preisach Model Parameters Based on an Improved Particle Swarm Optimization Method for Piezoelectric Actuators in Micro-Manufacturing Stages. *Micromachines*, **13**, Article No. 698. https://doi.org/10.3390/mi13050698

[92] Mayergoyz, I.D. and Friedman, G. (1988) Generalized Preisach Model of Hysteresis. *IEEE Transactions on Magnetics*, **24**, 212-217. https://doi.org/10.1109/20.43892

[93] Liu, V.-T. and Wing, H.-Y. (2022) Classical Preisach Model Based on Polynomial Approximation and Applied to Micro-Piezoelectric Actuators. *Symmetry*, **14**, Article No. 1008. https://doi.org/10.3390/sym14051008

[94] Szabó, Z. (2006) Preisach Functions Leading to Closed Form Permeability. *Physica B: Condensed Matter*, **372**, 61-67. https://doi.org/10.1016/j.physb.2005.10.020

[95] Mayergoyz, I.D. (1991) The Classical Preisach Model of Hysteresis. In: *Mathematical Models of Hysteresis*, Springer, New York, 1-63. https://doi.org/10.1007/978-1-4612-3028-1_1

[96] Banks, H.T., Kurdila, A.J. and Webb, G. (1997) Identification of Hysteretic Control Influence Operators Representing Smart Actuators Part I: Formulation. *Mathematical Problems in Engineering*, **3**, 287-328. https://doi.org/10.1155/S1024123X97000586

[97] Vojta, G. (2010) M. A. Krasnosel'skil, A. V. Pokrovskii. Systems with Hysteresis. Springer-Verlag, Berlin, Heidelberg, New York, London, Paris, Tokyo 1989, XVIII u. 410 S., 81 figures, DM 148.–, ISBN 3-540-15543-0. *Crystal Research and Technology*, **24**, K142. https://doi.org/10.1002/crat.2170240828

[98] Xu, R., Tian, D. and Wang, Z. (2020) Adaptive Tracking Control for the Piezoelectric Actuated Stage Using the Krasnosel'skii-Pokrovskii Operator. *Micromachines*, **11**, Article No. 537. https://doi.org/10.3390/mi11050537

[99] Li, Z., Shan, J. and Gabbert, U. (2018) Inverse Compensation of Hysteresis Using Krasnoselskii-Pokrovskii Model. *IEEE/ASME Transactions on Mechatronics*, **23**, 966-971. https://doi.org/10.1109/TMECH.2018.2805761

[100] Galinaitis, W.S. (1999) Two Methods for Modeling Scalar Hysteresis and Their Use in Controlling Actuators with Hysteresis. Doctoral Dissertation, Virginia Tech, Blacksburg.

[101] Amato, M., Ghezzi, L., Piegari, L. and Toscani, S. (2022) Definition and Identification of an Improved Preisach Model for Magnetic Hysteresis Based on the KP Operator. 2022 *IEEE International Instrumentation and Measurement Technology Conference* (*I2MTC*), Ottawa, 16-19 May 2022, 1-6. https://doi.org/10.1109/I2MTC48687.2022.9806703

[102] Egusa, S., *et al.* (2010) Multimaterial Piezoelectric Fibres. *Nature Materials*, **9**, 643-648. https://doi.org/10.1038/nmat2792

[103] Qin, Y., Xu, Y., Shen, C. and Han, J. (2022) High-Precision Displacement and Force Hybrid Modeling of Pneumatic Artificial Muscle Using 3D PI-NARMAX Model. *Actuators*, **11**, Article No. 51. https://doi.org/10.3390/act11020051

[104] Macki, J.W., Nistri, P. and Zecca, P. (1993) Mathematical Models for Hysteresis.

SIAM Review, **35**, 94-123. https://doi.org/10.1137/1035005

[105] Kuhnen, K. and Janocha, H. (2001) Inverse Feedforward Controller for Complex Hysteretic Nonlinearities in Smart-Material Systems. *Control and Intelligent Systems*, **29**, 74-83.

[106] Krikelis, K., van Berkel, K. and Schoukens, M. (2021) Artificial Neural Network Hysteresis Operators for the Identification of Hammerstein Hysteretic Systems. *IFAC-PapersOnLine*, **54**, 702-707. https://doi.org/10.1016/j.ifacol.2021.08.443

[107] Al-Bender, F., Symens, W., Swevers, J. and Van Brussel, H. (2004) Theoretical Analysis of the Dynamic Behavior of Hysteresis Elements in Mechanical Systems. *International Journal of Non-Linear Mechanics*, **39**, 1721-1735. https://doi.org/10.1016/j.ijnonlinmec.2004.04.005

[108] Li, S., Yang, X., Li, Y. and Liu, N. (2019) Research on Modelling of Piezoelectric Micro-Positioning Stage Based on PI Hysteresis Model. *The Journal of Engineering*, **2019**, 437-441. https://doi.org/10.1049/joe.2018.8978

[109] Hassani, V., Tjahjowidodo, T. and Do, T.N. (2014) A Survey on Hysteresis Modeling, Identification and Control. *Mechanical Systems and Signal Processing*, **49**, 209-233. https://doi.org/10.1016/j.ymssp.2014.04.012

[110] Lining, S., Changhai, R., Weibin, R., Liguo, C. and Minxiu, K. (2004) Tracking Control of Piezoelectric Actuator Based on a New Mathematical Model. *Journal of Micromechanics and Microengineering*, **14**, Article No. 1439. https://doi.org/10.1088/0960-1317/14/11/001

[111] Gan, J. and Zhang, X. (2014) A Novel Mathematical Piezoelectric Hysteresis Model Based on Polynomial. In: Zhang, X., Liu, H., Chen, Z. and Wang, N., Eds., *Intelligent Robotics and Applications. ICIRA* 2014. *Lecture Notes in Computer Science*, Vol. 8918, Springer, Cham, 354-365. https://doi.org/10.1007/978-3-319-13963-0_36

[112] Bashash, S. and Jalili, N. (2008) A Polynomial-Based Linear Mapping Strategy for Feedforward Compensation of Hysteresis in Piezoelectric Actuators. *Journal of Dynamic Systems, Measurement, and Control*, **130**, Article ID: 031008. https://doi.org/10.1115/1.2907372

[113] Yang, C., Verbeek, N., Xia, F., Wang, Y. and Youcef-Toumi, K. (2020) Modeling and Control of Piezoelectric Hysteresis: A Polynomial-Based Fractional Order Disturbance Compensation Approach. *IEEE Transactions on Industrial Electronics*, **68**, 3348-3358. https://doi.org/10.1109/TIE.2020.2977567

[114] Ikhouane, F., Mañosa, V. and Rodellar, J. (2005) Adaptive Control of a Hysteretic Structural System. *Automatica*, **41**, 225-231. https://doi.org/10.1016/j.automatica.2004.08.018

[115] Bouc, R. (1967) Forced Vibrations of Mechanical Systems with Hysteresis. *Proceedings of the* 4*th Conference on Non-linear Oscillations*, Prague, 5-9 September 1967.

[116] Wen, Y.-K. (1976) Method for Random Vibration of Hysteretic Systems. *Journal of the Engineering Mechanics Division*, **102**, 249-263. https://doi.org/10.1061/JMCEA3.0002106

[117] Coleman, B.D. and Hodgdon, M.L. (1987) On a Class of Constitutive Relations for Ferromagnetic Hysteresis. *Archive for Rational Mechanics and Analysis*, **99**, 375-396. https://doi.org/10.1007/BF00282052

[118] Banning, R., de Koning, W.L., Adriaens, H.J. and Koops, R.K. (2001) State-Space Analysis and Identification for a Class of Hysteretic Systems. *Automatica*, **37**, 1883-1892. https://doi.org/10.1016/S0005-1098(01)00157-1

[119] Su, C.-Y., Stepanenko, Y., Svoboda, J. and Leung, T.P. (2000) Robust Adaptive

Control of a Class of Nonlinear Systems with Unknown Backlash-Like Hysteresis. *IEEE Transactions on Automatic Control*, **45**, 2427-2432.

[120] Dahl, P.R. (1968) A Solid Friction Model. *The Aerospace Corporation*, **18**, 1-24.

[121] Zhang, B., Yuan, X., Zeng, Y., Lang, L., Liang, H. and Zhang, Y. (2022) Dahl Friction Model for Driving Characteristics of V-Shape Linear Ultrasonic Motors. *Micromachines*, **13**, Article No. 1407. https://doi.org/10.3390/mi13091407

[122] Xu, Q. and Li, Y. (2010) Dahl Model-Based Hysteresis Compensation and Precise Positioning Control of an XY Parallel Micromanipulator with Piezoelectric Actuation. *Journal of Dynamic Systems, Measurement, and Control*, **132**, Article ID: 041011. https://doi.org/10.1115/1.4001712

[123] Ahmad, I., Ali, M.A. and Ko, W. (2020) Robust μ-Synthesis with Dahl Model Based Feedforward Compensator Design for Piezo-Actuated Micropositioning Stage. *IEEE Access*, **8**, 141799-141813. https://doi.org/10.1109/ACCESS.2020.3013570

[124] Jiles, D.C. and Atherton, D.L. (1986) Theory of Ferromagnetic Hysteresis. *Journal of Magnetism and Magnetic Materials*, **61**, 48-60. https://doi.org/10.1016/0304-8853(86)90066-1

[125] Smith, R.C. and Ounaies, Z. (2000) A Domain Wall Model for Hysteresis in Piezoelectric Materials. *Journal of Intelligent Material Systems and Structures*, **11**, 62-79. https://doi.org/10.1106/HPHJ-UJ4D-E9D0-2MDY

[126] Rossi, C., Colorado, J., Coral, W. and Barrientos, A. (2011) Bending Continuous Structures with SMAs: A Novel Robotic Fish Design. *Bioinspiration & Biomimetics*, **6**, Article ID: 045005. https://doi.org/10.1088/1748-3182/6/4/045005

[127] Ikuta, K., Tsukamoto, M. and Hirose, S. (1991) Mathematical Model and Experimental Verification of Shape Memory Alloy for Designing Micro Actuator. *Proceedings of the* 1991 *IEEE Micro Electro Mechanical Systems*, Nara, 30 January-2 February 1991, 103-108.

[128] Vasanth, P., Kamalakannan, G.M. and Shivaraj, C.S. (2019) Study of Different Modelling Techniques of SMA Actuator and Their Validation through Simulation. In: Sridhar, V., Padma, M. and Rao, K., Eds., *Emerging Research in Electronics, Computer Science and Technology. Lecture Notes in Electrical Engineering*, Vol. 545, Springer, Singapore, 1211-1228. https://doi.org/10.1007/978-981-13-5802-9_104

[129] Önder, E.T., Sümer, B. and Başlamışlı, S.Ç. (2023) Estimation of Heat Transfer Model Parameters by Using Recursive Least Square (RLS) Method for a Shape Memory Alloy Wire. *Journal of Intelligent Material Systems and Structures*, **34**, 379-392. https://doi.org/10.1177/1045389X221105892

[130] Liu, Y., Liu, H., Wu, H. and Zou, D. (2016) Modelling and Compensation of Hysteresis in Piezoelectric Actuators Based on Maxwell Approach. *Electronics Letters*, **52**, 188-190. https://doi.org/10.1049/el.2015.3138

[131] Chen, J., Shang, H., Xia, D., Wang, S., Peng, T. and Zang, C. (2023) A Modified Vector Jiles-Atherton Hysteresis Model for the Design of Hysteresis Devices. *IEEE Transactions on Energy Conversion*. https://doi.org/10.1109/TEC.2023.3243101

[132] Li, Y., *et al.* (2023) Modified Jiles-Atherton Model for Dynamic Magnetization in X-Space Magnetic Particle Imaging. *IEEE Transactions on Biomedical Engineering*, **70**, 2035-2045. https://doi.org/10.1109/TBME.2023.3234256

[133] Benabou, A., Leite, J.V., Clenet, S., Simão, C. and Sadowski, N. (2008) Minor Loops Modelling with a Modified Jiles-Atherton Model and Comparison with the Preisach Model. *Journal of Magnetism and Magnetic Materials*, **320**, e1034-e1038. https://doi.org/10.1016/j.jmmm.2008.04.092

[134] Ru, C., Chen, L., Shao, B., Rong, W. and Sun, L. (2009) A Hysteresis Compensation Method of Piezoelectric Actuator: Model, Identification and Control. *Control Engineering Practice*, **17**, 1107-1114. https://doi.org/10.1016/j.conengprac.2009.04.013

[135] Chuntao, L. and Yonghong, T. (2004) A Neural Networks Model for Hysteresis Nonlinearity. *Sensors and Actuators A*: *Physical*, **112**, 49-54. https://doi.org/10.1016/j.sna.2003.11.016

[136] Dong, R., Tan, Y., Hui, C. and Xie, Y. (2008) A Neural Networks Based Model for Rate-Dependent Hysteresis for Piezoceramic Actuators. *Sensors and Actuators A*: *Physical*, **143**, 370-376. https://doi.org/10.1016/j.sna.2007.11.023

[137] Yang, C.-H. and Chang, K.-M. (2006) Adaptive Neural Network Control for Piezoelectric Hysteresis Compensation in a Positioning System. 2006 *IEEE International Symposium on Industrial Electronics*, Montreal, 9-13 July 2006, 829-834. https://doi.org/10.1109/ISIE.2006.295742

[138] Quondam-Antonio, S., Riganti-Fulginei, F., Laudani, A., Lozito, G.-M. and Scorretti, R. (2023) Deep Neural Networks for the Efficient Simulation of Macro-Scale Hysteresis Processes with Generic Excitation Waveforms. *Engineering Applications of Artificial Intelligence*, **121**, Article ID: 105940. https://doi.org/10.1016/j.engappai.2023.105940

[139] Zou, Y. and Wang, B. (2006) Fragmental Ellipse Fitting Based on Least Square Algorithm. *Chinese Journal of Scientific Instrument*, **27**, 808-812. (In Chinese)

[140] Han, W., Shao, S., Zhang, S., Tian, Z. and Xu, M. (2022) Design and Modeling of Decoupled Miniature Fast Steering Mirror with Ultrahigh Precision. *Mechanical Systems and Signal Processing*, **167**, Article ID: 108521. https://doi.org/10.1016/j.ymssp.2021.108521

[141] Meng, Y., Zhao, K. and Guo, P. (2022) Experimental Investigation of Coupled Hysteretic Thermo-Electro-Mechanical Properties of Piezo Stack Actuator. In: Wang, Y., Martinsen, K., Yu, T. and Wang, K., Eds., *Advanced Manufacturing and Automation XI. IWAMA* 2021. *Lecture Notes in Electrical Engineering*, Vol. 880, Springer, Singapore, 466-471. https://doi.org/10.1007/978-981-19-0572-8_59

[142] Feng, Y., Hu, Z. and Liang, M. (2023) Modelling of Piezoelectric Actuating Systems Subjected to Variable Loads and Frequencies and Applications to Prescribed Performance Control. *International Journal of Control*, **96**, 2356-2373. https://doi.org/10.1080/00207179.2022.2094836

[143] Habibullah, H. (2020) 30 Years of Atomic Force Microscopy: Creep, Hysteresis, Cross-Coupling, and Vibration Problems of Piezoelectric Tube Scanners. *Measurement*, **159**, Article ID: 107776. https://doi.org/10.1016/j.measurement.2020.107776

[144] Mörée, G. and Leijon, M. (2023) Review of Hysteresis Models for Magnetic Materials. *Energies*, **16**, Article No. 3908. https://doi.org/10.3390/en16093908

[145] Chen, J., Peng, G., Hu, H. and Ning, J. (2020) Dynamic Hysteresis Model and Control Methodology for Force Output Using Piezoelectric Actuator Driving. *IEEE Access*, **8**, 205136-205147. https://doi.org/10.1109/ACCESS.2020.3037216

[146] Rupnik, U., Alić, A. and Miljavec, D. (2022) Harmonization and Validation of Jiles-Atherton Static Hysteresis Models. *Energies*, **15**, Article No. 6760. https://doi.org/10.3390/en15186760

[147] Zhou, C., Feng, C., Aye, Y.N. and Ang, W.T. (2021) A Digitized Representation of the Modified Prandtl-Ishlinskii Hysteresis Model for Modeling and Compensating Piezoelectric Actuator Hysteresis. *Micromachines*, **12**, Article No. 942. https://doi.org/10.3390/mi12080942

[148] Zhang, S., Zhao, H., Ma, X., Deng, J. and Liu, Y. (2022) A 3-DOF Piezoelectric Mi-

cromanipulator Based on Symmetric and Antisymmetric Bending of a Cross-Shaped Beam. *IEEE Transactions on Industrial Electronics*, **70**, 8264-8275. https://doi.org/10.1109/TIE.2022.3213906

[149] Sabarianand, D.V., Karthikeyan, P. and Muthuramalingam, T. (2020) A Review on Control Strategies for Compensation of Hysteresis and Creep on Piezoelectric Actuators Based Micro Systems. *Mechanical Systems and Signal Processing*, **140**, Article ID: 106634. https://doi.org/10.1016/j.ymssp.2020.106634

[150] Li, J., Zhang, L., Li, S., Mao, Q. and Mao, Y. (2023) Active Disturbance Rejection Control for Piezoelectric Smart Structures: A Review. *Machines*, **11**, Article No. 174. https://doi.org/10.3390/machines11020174

[151] Qin, Y., Tian, Y., Zhang, D., Shirinzadeh, B. and Fatikow, S. (2013) A Novel Direct Inverse Modeling Approach for Hysteresis Compensation of Piezoelectric Actuator in Feedforward Applications. *IEEE/ASME Transactions on Mechatronics*, **18**, 981-989. https://doi.org/10.1109/TMECH.2012.2194301

[152] Qin, Y., Duan, H. and Han, J. (2021) Direct Inverse Hysteresis Compensation of Piezoelectric Actuators Using Adaptive Kalman Filter. *IEEE Transactions on Industrial Electronics*, **69**, 9385-9395. https://doi.org/10.1109/TIE.2021.3114741

[153] Rakotondrabe, M. (2010) Bouc-Wen Modeling and Inverse Multiplicative Structure to Compensate Hysteresis Nonlinearity in Piezoelectric Actuators. *IEEE Transactions on Automation Science and Engineering*, **8**, 428-431. https://doi.org/10.1109/TASE.2010.2081979

[154] Qin, Y., Zhang, Y., Duan, H. and Han, J. (2021) High-Bandwidth Hysteresis Compensation of Piezoelectric Actuators via Multilayer Feedforward Neural Network Based Inverse Hysteresis Modeling. *Micromachines*, **12**, Article No. 1325. https://doi.org/10.3390/mi12111325

[155] Ang, W.T., Khosla, P.K. and Riviere, C.N. (2007) Feedforward Controller with Inverse Rate-Dependent Model for Piezoelectric Actuators in Trajectory-Tracking Applications. *IEEE/ASME Transactions on Mechatronics*, **12**, 134-142. https://doi.org/10.1109/TMECH.2007.892824

[156] Dong, R., Tan, Y., Xie, Y. and Li, X. (2023) A Dynamic Hysteresis Model of Piezoelectric Ceramic Actuators. *Chinese Journal of Electronics*, **32**, 1-8.

[157] Zhong, B., Liu, S., Wang, C., Jin, Z. and Sun, L. (2023) A Novel Feedforward Model of Piezoelectric Actuator for Precision Rapid Cutting. *Materials*, **16**, Article No. 2271. https://doi.org/10.3390/ma16062271

[158] An, D., *et al*. (2023) Compensation Method for the Nonlinear Characteristics with Starting Error of a Piezoelectric Actuator in Open-Loop Controls Based on the DSPI Model. *Micromachines*, **14**, Article No. 742. https://doi.org/10.3390/mi14040742

[159] Wu, Y., Chen, H., Sun, N., Fan, Z. and Fang, Y. (2023) Neural Network Based Adaptive Control for a Piezoelectric Actuator with Model Uncertainty and Unknown External Disturbance. *International Journal of Robust and Nonlinear Control*, **33**, 2251-2272. https://doi.org/10.1002/rnc.6517

[160] Savoie, M. and Shan, J. (2022) Temperature-Dependent Asymmetric Prandtl-Ishlinskii Hysteresis Model for Piezoelectric Actuators. *Smart Materials and Structures*, **31**, Article ID: 055022. https://doi.org/10.1088/1361-665X/ac6552

[161] Baziyad, A.G., Nouh, A.S., Ahmad, I. and Alkuhayli, A. (2022) Application of Least-Squares Support-Vector Machine Based on Hysteresis Operators and Particle Swarm Optimization for Modeling and Control of Hysteresis in Piezoelectric Actuators. *Actuators*, **11**, Article No. 217. https://doi.org/10.3390/act11080217

[162] Ji, H.-W., *et al*. (2023) Modeling and Control of Rate-Dependent Hysteresis Cha-

racteristics of Piezoelectric Actuators Based on Analog Filters. *Ferroelectrics*, **603**, 94-115. https://doi.org/10.1080/00150193.2022.2159223

[163] Li, W., Liu, K., Yang, Z. and Wang, W. (2022) Dynamic Modeling and Disturbance Rejection Compensation for Hysteresis Nonlinearity of High Voltage Piezoelectric Stack Actuators. *Smart Materials and Structures*, **32**, Article ID: 025007. https://doi.org/10.1088/1361-665X/acad4e

[164] Gu, G.-Y., Yang, M.-J. and Zhu, L.-M. (2012) Real-Time Inverse Hysteresis Compensation of Piezoelectric Actuators with a Modified Prandtl-Ishlinskii Model. *Review of Scientific Instruments*, **83**, Article ID: 065106. https://doi.org/10.1063/1.4728575

[165] Ko, Y.-R., Hwang, Y., Chae, M. and Kim, T.-H. (2017) Direct Identification of Generalized Prandtl-Ishlinskii Model Inversion for Asymmetric Hysteresis Compensation. *ISA Transactions*, **70**, 209-218. https://doi.org/10.1016/j.isatra.2017.07.004

[166] Lallart, M., Li, K., Yang, Z., Zhou, S. and Wang, W. (2020) Simple and Efficient Inverse Hysteretic Model and Associated Experimental Procedure for Precise Piezoelectric Actuator Control and Positioning. *Sensors and Actuators A*: *Physical*, **301**, Article ID: 111674. https://doi.org/10.1016/j.sna.2019.111674

[167] Zhang, Q., Gao, Y., Li, Q. and Yin, D. (2021) Adaptive Compound Control Based on Generalized Bouc-Wen Inverse Hysteresis Modeling in Piezoelectric Actuators. *Review of Scientific Instruments*, **92**, Article ID: 115004. https://doi.org/10.1063/5.0059368

[168] Son, N.N., Van Kien, C. and Anh, H.P.H. (2022) Adaptive Sliding Mode Control with Hysteresis Compensation-Based Neuroevolution for Motion Tracking of Piezoelectric Actuator. *Applied Soft Computing*, **115**, Article ID: 108257. https://doi.org/10.1016/j.asoc.2021.108257

[169] Tan, U.-X., Win, T. and Ang, W.T. (2006) Modeling Piezoelectric Actuator Hysteresis with Singularity Free Prandtl-Ishlinskii Model. 2006 *IEEE International Conference on Robotics and Biomimetics*, Kunming, 17-20 December 2006, 251-256. https://doi.org/10.1109/ROBIO.2006.340162

[170] Yang, X., Li, W., Wang, Y., Ye, G. and Su, X. (2009) Hysteresis Modeling of Piezo Actuator Using Neural Networks. 2008 *IEEE International Conference on Robotics and Biomimetics*, Bangkok, 22-25 February 2009, 988-991. https://doi.org/10.1109/ROBIO.2009.4913134

[171] Gan, J., Zhang, X. and Wu, H. (2016) Tracking Control of Piezoelectric Actuators Using a Polynomial-Based Hysteresis Model. *AIP Advances*, **6**, Article ID: 065204. https://doi.org/10.1063/1.4953597

[172] Al Janaideh, M. and Aljanaideh, O. (2018) Further Results on Open-Loop Compensation of Rate-Dependent Hysteresis in a Magnetostrictive Actuator with the Prandtl-Ishlinskii Model. *Mechanical Systems and Signal Processing*, **104**, 835-850. https://doi.org/10.1016/j.ymssp.2017.09.004

[173] Tao, Y.-D., Li, H.-X. and Zhu, L.-M. (2019) Rate-Dependent Hysteresis Modeling and Compensation of Piezoelectric Actuators Using Gaussian Process. *Sensors and Actuators A*: *Physical*, **295**, 357-365. https://doi.org/10.1016/j.sna.2019.05.046

[174] Al Janaideh, M., Al Saaideh, M. and Rakotondrabe, M. (2020) On Hysteresis Modeling of a Piezoelectric Precise Positioning System under Variable Temperature. *Mechanical Systems and Signal Processing*, **145**, Article ID: 106880. https://doi.org/10.1016/j.ymssp.2020.106880

[175] Wang, W., *et al.* (2020) Research on Asymmetric Hysteresis Modeling and Compensation of Piezoelectric Actuators with PMPI Model. *Micromachines*, **11**, Article

No. 357. https://doi.org/10.3390/mi11040357

[176] Shan, X., Song, H., Cao, H., Zhang, L., Zhao, X. and Fan, J. (2021) A Dynamic Hysteresis Model and Nonlinear Control System for a Structure-Integrated Piezoelectric Sensor-Actuator. *Sensors*, **21**, Article No. 269. https://doi.org/10.3390/s21010269

[177] Xu, M., Su, L.-R. and Chen, S.-T. (2023) Improved PI Hysteresis Model with One-Sided Dead-Zone Operator for Soft Joint Actuator. *Sensors and Actuators A: Physical*, **349**, Article ID: 114072. https://doi.org/10.1016/j.sna.2022.114072

[178] Feng, Y. and Li, Y. (2020) System Identification of Micro Piezoelectric Actuators via Rate-Dependent Prandtl-Ishlinskii Hysteresis Model Based on a Modified PSO Algorithm. *IEEE Transactions on Nanotechnology*, **20**, 205-214. https://doi.org/10.1109/TNANO.2020.3034965

[179] Louis, A., Valérie, P.-B. and Joël, B.-G. (2023) Comparison of Control Strategies for Hysteresis Attenuation in Electromechanical Actuators Subject to Dispersion. *Control Engineering Practice*, **130**, Article ID: 105348. https://doi.org/10.1016/j.conengprac.2022.105348

[180] Zhang, Y., Wu, J., Huang, P., Su, C.-Y. and Wang, Y. (2023) Inverse Dynamics Modelling and Tracking Control of Conical Dielectric Elastomer Actuator Based on GRU Neural Network. *Engineering Applications of Artificial Intelligence*, **118**, Article ID: 105668. https://doi.org/10.1016/j.engappai.2022.105668

[181] Yang, L., Zhao, Z., Zhang, Y. and Li, D. (2021) Rate-Dependent Modeling of Piezoelectric Actuators for Nano Manipulation Based on Fractional Hammerstein model. *Micromachines*, **13**, Article No. 42. https://doi.org/10.3390/mi13010042